MASTER THESIS

Thesis submitted in partial fulfillment of the requirements for the degree of Master of Science in Engineering at the University of Applied Sciences Technikum Wien – Degree Program Tissue Engineering and Regenerative Medicine

Understanding the Requirements for Viability in Absence of Mitochondrial DNA

By: Ludwig Karl, BSc
Student Number: te16m036

Supervisor 1: Genya Frenkel, Ph. D
Supervisor 2: Mag. Dr. Thomas Machacek

Vienna, 30.09.2019

FH University of Applied Sciences
TECHNIKUM WIEN

Declaration of Authenticity

“As author and creator of this work to hand, I confirm with my signature knowledge of the relevant copyright regulations governed by higher education acts (for example see §§ 21, 42f and 57 UrhG (Austrian copyright law) as amended as well as § 14 of the Statute on Studies Act Provisions / Examination Regulations of the UAS Technikum Wien).

In particular I declare that I have made use of third-party content correctly, regardless what form it may have, and I am aware of any consequences I may face on the part of the degree program director if there should be evidence of missing autonomy and independence or evidence of any intent to fraudulently achieve a pass mark for this work (see § 14 para. 1 Statute on Studies Act Provisions / Examination Regulations of the UAS Technikum Wien).

I further declare that up to this date I have not published the work to hand, nor have I presented it to another examination board in the same or similar form. I affirm that the version submitted matches the version in the upload tool.”

Vienna, 01.09.2019

Place, Date

Signature

Abstract

Mitochondria are well known as the “powerhouse of the cell”, but they regulate substantially more than just energy generation via the oxidative phosphorylation system. Mitochondria are environmental sensors, interact directly within the cells cytosol to activate pathways upon a specific metabolic trigger and are the main source for all major bioenergetic compounds in order to sustain stress, promote longevity and keeping homeostasis of the energy flow of the body. This project is based on a major genome wide CRISPR screen of nearly 20 thousand human genes on a specific phenotype of interest, which identified several promising hits, suggesting novel functions of genes associated with the mitochondrial electron transport chain. We utilized the basic notion of the CRISPR screen and repeated the conditions in order to validate each specific hit within the boundaries of a fluorescence-activated cell sorting based death screen. Additionally, seahorse assays were used to observe the phenotype and the underlying effects of the specific knockouts in 143B cells. Moreover, we aimed to establish a new multi guide vector by using golden gate cloning to develop a tool capable of knocking out the mitochondrial polymerase. This procedure aims to generate a population which can then be split between different treatments in which mtDNA may be more or less essential. 3 out of 4 hits were confirmed and subjected to western blotting and immunostainings to further analyze the predicted novel function of respective genes. The multi guide vector system has been successfully established but has yet to be proven more efficient and robust than common lentiviral co-transduction as well as transient co-transfection methods. We discovered additional, yet unknown, functions of 3 genes which have never been associated with the mitochondrial oxidative phosphorylation system before. Further investigations are going to elucidate their importance in cellular respiration and contribute to a better understanding of mitochondria associated degenerative diseases.

Keywords: mtDNA, CRISPR, FACS, OXPHOS, mitochondria, rho 0

Abstract (German)

Mitochondrien sind bekanntlich die Kraftwerke aller somatischen- und Keimbahnzellen, regulieren jedoch bei weitem mehr als den Energiehaushalt, welcher mittels der oxidativen Phosphorylierung stattfindet. Mitochondrien fungieren ebenfalls als Umweltsensoren, interagieren innerhalb des Zytosols der Zelle mit weiteren Organellen um Signalwege zu aktivieren, welche durch eine Vielfalt von Metaboliten und Liganden ausgelöst werden. Zusätzlich sind sie der Hauptproduzent der wichtigsten bioenergischen Substanzen, um zellulären Stress zu überbrücken, Langlebigkeit zu gewährleisten und den Körper in Homeostase zu halten. Die folgende Arbeit basiert auf einem umfassenden genetischen CRISPR Screen von zwanzigtausend menschlichen Genen, die einen spezifischen Phänotypen analysiert haben. Dadurch wurden mehrere Kandidatengene erstmals mit zellulärer Respiration in Verbindung gebracht, was auf unaufgekärte Funktionen hinweist. Diese Funktionen sind mit der mitochondrialen Elektronentransportkette assoziiert und stellen daher eine Schlüsselfunktion unseres Stoffwechsels dar. Wir nutzten die Grundprinzipien des CRISPR Screens und wiederholten diesen mit den identischen Konditionen mittels eines FACS Death Screens, um die spezifischen Kandidatengene einzelnd zu validieren. Zusätzlich untersuchten wir die Respirationskapazitäten der einzelnen 143B knock-out Zelllinien mittels Seahorse Assays. Ein weiteres Ziel bestand darin einen mehrfach guide Vector mittels golden gate Klonierung zu entwickeln, welcher die Genexpression der mitochondrialen Polymerase ausschalten soll. 3 von 4 hits wurden verifiziert und Western blotting, sowie immunohistologischen Färbungen, unterzogen, um die Prognose neuer Funktionen und zusätzlicher Lokalisation der expressionierten Proteine zu analysieren. Der mehrfach guide Vector wurde erfolgreich generiert, muss jedoch noch auf seine Effizients und Robustheit geprüft werden. Diese Arbeit schildert die Entdeckung zusätzlicher Funktionen von 3 Genen, welche erstmals mit der mitochondrialen oxidativen Phosphorylierung in Verbindung gebracht wurde. Zukünftige Studien dieser Gene werden deren Rolle in der zellulären Respiration aufdecken und ein besseres Verständnis über mitochondrial assoziierte degenerative Krankheiten darlegen.

Keywords: mtDNA, CRISPR, FACS, OXPHOS, mitochondrion, rho 0

Disclaimer

This master thesis documents several important results of an ongoing project, which revealed novel gene functions. Therefore, the Whitehead Institute classified this thesis in part. Gene names are pseudonymized and further details about general functions, as well as the involvement of respective genes in disease and metabolism, are withhold.

Table of Contents

1 Introduction

Mitochondria play a key role in the regulation and production of cellular bioenergetics; furthermore, they are the primary source of producing the majority of adenosine triphosphate molecules by utilizing the oxidative phosphorylation system (OXPHOS). Additionally, mitochondria and the respectively embedded OXPHOS are playing a crucial role in the plasticity, development, differentiation and proliferation of neurons. The impairment of various mitochondrial functions has been noted in a major set of general psychiatric and phenotypical disorders, constraining schizophrenia (SCZ), a devastating and chronic condition that seriously impacts every aspect of the life's of patients and their surroundings [1]. Evidence collected in recent decades in imaging, transcriptomic, proteomic and metabolomic studies indicate a contribution of the OXPHOS deficit in SCZ and related psychiatric disorders, such as bipolar, anxiety/panic, schizotypal personality and delusional disorders [2], [3]. Disturbed mitochondrial function is also implicated in mitochondrial myopathy a disorder known to cause a subset of systemic disorders such as neuromuscular diseases, which is based on impaired OXPHOS leading to a lack of energy and results into severe weakness of limbs and muscle tenderness [4], [5]. The majority of the energy sources necessary for proper cell functioning are based on oxidative phosphorylation in the internal mitochondrial membrane. Damaged mitochondria release substantial amounts of reactive oxygen species, which are normally tightly controlled by mitochondrial permeability transition pores (mPTP), also known as opening-associated ROS release mechanisms and constitute a regenerative cycle of mitochondrial ROS formation [6], [7]. Similarly, reducing the activity of antioxidant enzymes (e.g. glutathione, and superoxide dismutase (SOD) increases the production of reactive oxygen species [8]. About 16.5 kb of circular mitochondrial DNA is contained in specialized nucleoids throughout the mitochondrial matrix and comprises (up to this date) 37 genes in total, which are responsible for encoding 13 proteins, 22 tRNAs and 2 rRNAs. These 13 proteins enforce the cell to produce subunits of the mitochondrial respiratory chain complex in order to enable the oxidative phosphorylation machinery [9], [10]; thus, playing a crucial role of maintaining and facilitating cellular respiration within each single somatic and germ cell. In order to further understand the key role of mitochondria in heterotrophic organisms we have to elucidate their role as the well-known "powerhouse of the cell" by discussing the underlying energy generating pathways and breaking points, causing several dysfunctions and disorders [2], [3].

1.1 Cellular Respiration and Underlying Diseases

Cellular respiration is the process of utilizing oxygen and glucose in order to generate ATP and is used by heterotrophs and partially autotrophs, which are obtaining organic compounds in the presence of oxygen and converting it into CO_2, H_2O and ATP. There are 3 major steps in cellular respiration, the first is glycolysis, the second one is known as Krebs cycle and the third step, which is generating the majority of ATP in the human body, the electron transport chain [11].

1.1.1 Glycolysis

The process of glycolysis (Figure 1) occurs outside of the mitochondria, namely in the cytoplasm of each individual cell. During Glycolysis the 6-carbon glucose molecule is broken down into two molecules of pyruvate, which consists of 3 carbons. Additionally, 2 molecules of ATP and 2 molecules of NADH (due to the reduction of NAD^+) are released as well. At the start of glycolysis, glucose is phosphorylated, facilitated by the hexokinase and its cofactor Mg^{2++} to generate glucose 6-phosphate. Afterwards, phosphoglucose isomerase generates fructose 6- phosphate, which is subjected to the phosphofructokinase generating fructose biphosphate [11], [12]. The next step includes the “lysing” of the phosphorylated fructose molecule by fructose biphosphate aldolase resulting in two 3 carbon chains of glycerolaldehyde 3- phosphate. Later on, glyceraldehyde dehydrogenase facilitates the addition of another phosphate group to the glyceraldehyde molecule by using NAD^+ and Mg^{2++} to catalyze the reaction. Phosphoglycerade kinase removes one phosphate group and produces 1 ATP molecule, whereas phosphoglycerate mutase, a class of isomerases, shifts the residual phosphate group from position C-3 to C-2, resulting into 2 phosphoglycerate molecules. This enables the enzyme enolase to catalyze 2- phosphoglycerate to phosphoenolpyruvate. At last, pyruvate kinase catalyzes the generation of pyruvate from phosphoenolpyruvate by producing another 2 ATP molecules [11].

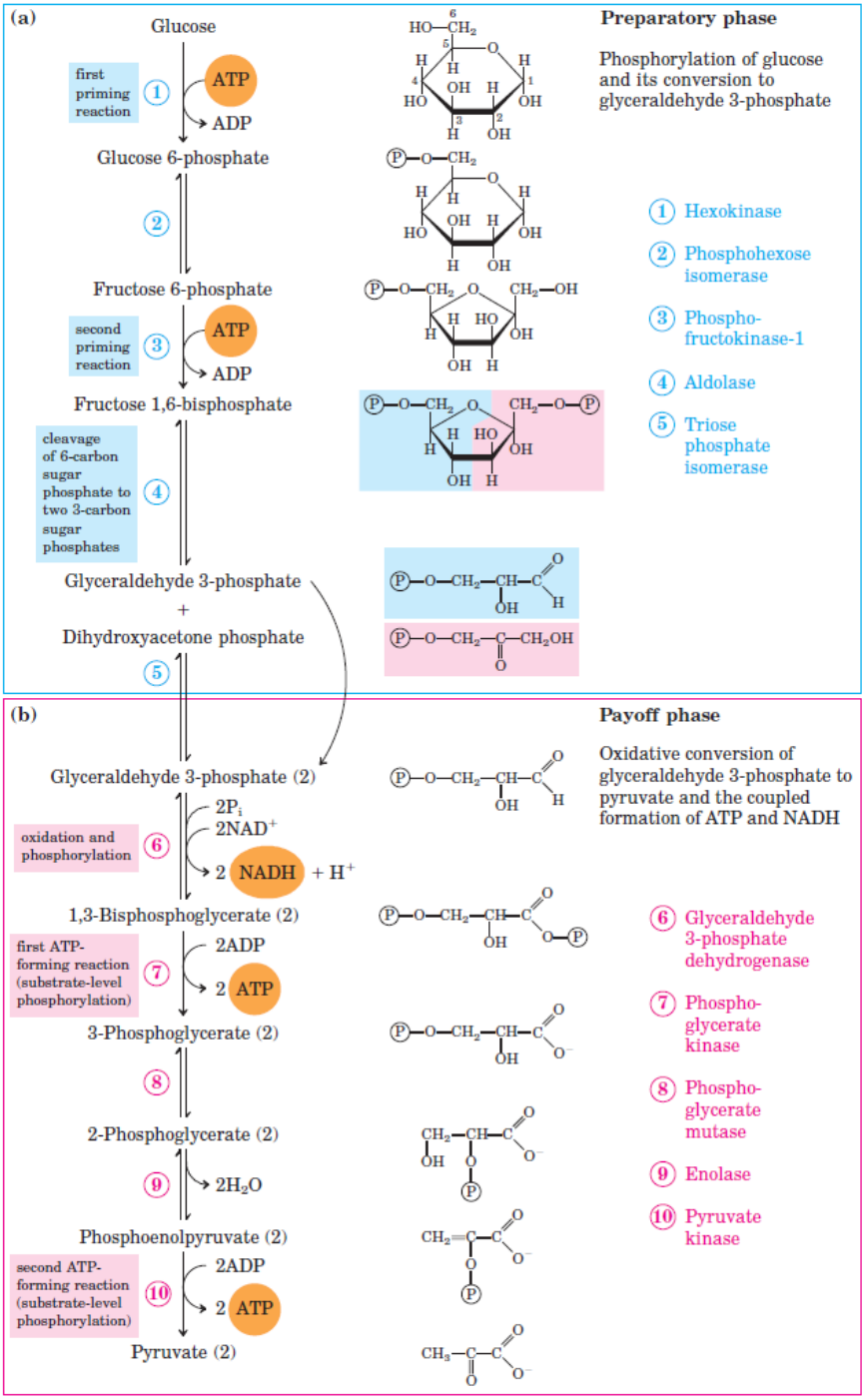

Figure 1, Glycolysis. Separated by 2 distinct phases, (a) the preparatory phase where 2 ATP molecules are invested and (b) the payoff phase where 2 NADH and 4 ATP molecules are generated [12 - Accesed 7-10-2019]

1.1.2 Pyruvate Metabolism

Pyruvate is one of the most important molecules destined to act as key intermediate in various metabolic pathways. It can transform itself through a chemical reaction into 1 of 4 different products depended on the energetic state within the cell [13]. The first pathway pyruvate can take is to convert into lactic acid. This pathway is also known as anaerobic

glycolysis. Glycolysis and all other metabolic pathways have one goal in common, namely, to work in tandem to form reactants and cofactors that can be used with one another to ultimately feed into the electron transport chain to generate an abundance of ATP [13], [14]. The enzyme converting pyruvate into lactic acid is called lactate dehydrogenase (LDH). This enzyme is only active in conditions such as low oxygen states, where it utilizes cofactor B3. Clinically, low oxygen states occur in infection, hypoxia, ischemia and cardiac arrest and correlates with lactate levels in the blood, which constitutes a critical indicator, that tissue does not have adequate oxygenation, indicating possible occurrences of prior mentioned events [15]. In certain tissues such as testes, lens, cornea, medulla, white blood cells and red blood cells lactic acid has a propensity to occur. Another possible pathway for pyruvate is to be transformed into alanine. This conversion is known as alanine aminotransferase pathway conducted by the alanine aminotransferase (ALT) and its cofactor vitamin B6 [15], [16]. The Cahill cycle acts as series of reactions to transport carbon and amino groups from muscle to liver. In order to recycle carbons between muscle and liver pyruvate has to be converted to alanine, or glucose (via gluconeogenesis). The Cahill cycle starts with the conversion of pyruvate to alanine by utilizing glutamate, which is converted to α-ketoglutarate (α-KG) [17]. Pyruvate can not be transferred between muscle and liver, but alanine can. Once alanine is converted within the muscle, it can be transported to the liver where it will be converted into pyruvate by using α-KG and subsequently producing alanine and glutamate. Pyruvate is used for gluconeogenesis in the liver and the glucose is then transported to the muscle ultimately producing pyruvate again in order to close the cycle [11], [15]. The Cahill cycle is the constant conversion of pyruvate to alanine, alanine to pyruvate, pyruvate to glucose and glucose to pyruvate, aiming to utilize the carbons provided by pyruvate for further metabolic pathways; the Cahill cycle and the production of lactic acid takes place in the cytosol, whereas the following 2 pathways are catalyzed within mitochondria. Another pathway for pyruvate is the conversion to oxaloacetate by using pyruvate carboxylase and biotin as cofactor [17]. Oxaloacetate is an important reactant used for gluconeogenesis and the Krebs Cycle and acts as a failsafe mechanism to push the reaction into the preferred state. The most important conversion of pyruvate is the conversion to acetyl coenzyme A by pyruvate dehydrogenase (PDH), the main reactant of the Krebs cycle. It is used to initiate the Krebs cycle and generate the carbon dioxide necessary to carry out a series of reactions that in unison across all reactions will ultimately make use of all the products to feed into the electron transport chain to generate ATP [11].

1.1.3 The Krebs Cycle

The Krebs cycle takes place in the inner matrix of the mitochondria and starts after pyruvate is generated during glycolysis. Pyruvate diffuses into the mitochondrial matrix and builds up the pyruvate dehydrogenase complex (PDH complex), which is converted into acetyl coenzyme A (acetyl-CoA), a 2-carbon molecule [14]. The remainder carbon molecule is released by the mitochondria as CO_2 due to the decarboxylation process. Acetyl-CoA reacts with a four-carbon compound called oxaloacetic acid to form the 6-carbon acid carbon molecule and a molecule of CO_2 is formed reducing the eventual product to a 5-carbon product. In the process, a NADH and H+ is produced and another molecule of CO_2 is released. In order to form the 4-carbon compound oxaloacetic acid $FADH_2$, ATP and another NADH molecule is produced [11]. There are several documented disorders associated with

the Krebs Cycle, 2-oxoglutaric aciduria, fumarase deficiency and succinyl-CoA synthetase (SCS) deficiency, which is highly affecting mitochondrial functions and sustainment. Oxoglutaric aciduria is a rare autosomal recessive disease, shows an early neonatal onset and is associated with PDH complex deficiency, triggering hypotonia, seizures and results into neurodegenerative phenotypes [18], [19]. It is mitochondrially encoded and mediates the decarboxylation process of α-KG. Interestingly, fumarate deficiency and SCS deficiency are both diseases resulting into impaired neuronal development, are mainly described as an encephalomyopathy phenotype and are mitochondrially encoded as well [11], [14], [18]–[20].

1.1.4 Electron Transport Chain

During the final step of ATP production high energy NAD^+ and $FADH_2$ delivers their electrons to the electron transport chain by moving through a series of proteins, which are pumping protons into the intermembrane space of the mitochondria. The electrons are captured by the electron acceptor oxygen; due to the hyperpolarization of the inner mitochondrial membrane, backflowing proton are utilized by ATPase motor protein to generate ATP resulting in H_20 as byproduct. This results into 32 ATP molecules [11].

The electron transport chain consists of 4 important proteins known as complex I (NADH dehydrogenase), II (Succinate Dehydrogenase), III (Cytochrome C Oxireductase and IV (Cytochrome Oxidase). The two major substrates to initiate the oxidative phosphorylation process are electron carriers, obtained from prior described glycolysis and Krebs cycle. Complex I consist of flavoinmononucleotide (FMN) a vitamin B2 derivative and several iron sulfur centers to carry electrons [11]. It is the largest multi subunit complex and associated with several degenerative and hereditary disorders. For example, Complex I linked deficiency is caused by several mutations within nuclear and mtDNA and can occur during adulthood and childhood, which states a severe problem for clinical diagnosis, because of the contribution of two genomes (nuclear and mitochondrial) [11], [21]. Typical phenotypes of complex I linked deficiency are, stroke-like episodes, hypertrophic cardiomyopathy, mitochondrial encephalomyopathy and an early onset of Leigh syndrome causing an ongoing exponentially impairment of patients motoric and mental abilities [21].

Another important mobile protein structure, which diffuses into the inner mitochondrial membrane and serving as electron carrier, is ubiquinone, also known as Coenzyme Q10 (CoQ10). CoQ10 is widely used as efficient supplement in order to treat a variety of mitochondrial diseases and stalling the destructive path of neurodegenerative disorders such as Huntington's, or Parkinson's disease [22]. Although several studies showed significant results of CoQ10 supplementation, it is highly debated if CoQ10 supplementation may counteract the various aging associated diseases overall. Cardiovascular diseases, hypertension, periodontal infection, atherosclerosis and neurodegenerative diseases are interestingly corresponding with low CoQ10 levels and proximate oral supplementation is capable of reducing inflammatory markers and may counteract attenuation of impaired mitochondrial functions [23], [24].

At the start of oxidative phosphorylation, the enzyme NADH dehydroxynase oxidizes $NADH^+$ to NAD and obtains 2 electrons through this process. These 2 electrons are transferred to

FMN within complex I, passing through a series of iron-sulfur structures, where it will stop at the iron sulfur center. This will facilitate the initiation of the proton gradient by coupling the electron transfer with transmembrane proton pumping [11]. As the two H+ protons bind to ubiquitin creating the ubiquinol molecule, 4 H+ molecules diffuse into the intermembrane space. Ubiquinol travels through the inner mitochondrial membrane, passing complex II and associates with complex III. Another severe disease associated with the electron transport chain is also known as mitochondrial complex II deficiency (succinate dehydrogenase deficiency) [25]. It is known as an autosomal recessive disorder and comprises a multitude of possible phenotypes. Compared to complex I deficiency, all four subunits are nuclear encoded. It is classified as congenital disorder of metabolism and results into similar phenotypes such as complex I deficiency with higher negative impact on neuronal development and cerebellar atrophy. Interestingly, Complex II participates in the Krebs cycle and electron transport chain by catalyzing the oxidation of succinate to fumarate by coupling the reduction of ubiquinone to ubiquinol [25].

Complex III is comprised of 3 important structures, cytochrome b, rieske iron-sulfur proteins and cytochrome c. Cytochrome c is a mobile protein within the inter membrane space and is attached to complex III. During the oxidation of ubiquinol to ubiquinone, mediated by complex III, 2 of its electrons are passed to cytochrome c and 4 H+ protons diffuse through complex III into the intermembrane space, building up the electro chemical gradient. Afterwards, cytochrome c travels through the inter membrane space and passes 2 electrons to complex IV, which reduces ½ O_2 with two hydrogen ions to generate one H_2O molecule [11]. During this process, two additional protons are pumped into the inter membrane space. In total 10 H+ protons are being pumped into the intermembrane space by the initiation of the electron transport of the NADH molecule. Concentration gradients are a key component of the biological world, because the potential energy from these gradients are often used to perform biological work. In this case, the ATP synthase will generate ATP from ADP + Pi when the hydrogen protons, located in high concentrations in the intermembrane, backflow into the low concentration mitochondrial matrix [11], [15].

1.2 Evolution of Mitochondria

Mitochondria are double membrane organelles consisting of the intermembrane, outer membrane and in between the intermembrane space. Mitochondria used to be bacteria on their own, because they reproduce by binary fission, used to have their own DNA and ribosomes [9], [26]. An interesting fact is that a great proportion of the nuclear encoded proteins where originally mitochondrial encoded. Mitochondria arose about 2 billion years ago during an endosymbiotic event in which an archaea bacteria, which possessed a nucleus, engulfed another proteobacteria [27], [28]. These bacteria derived from the eubacterial kingdom, resisted the digestive attempts of the archaea and thereby, the symbiosis created a new organism of acquired two sets of DNA. The eubacterial DNA, which was engulfed proceeded to lose quite rapidly most of its DNA but kept synergistic metabolic processes. Most of its DNA is speculated to be completely lost, because of a redundancy with the DNA already present in the engulfing bacteria and some of it was transferred (via horizontal gene transfer) to the other genome [28]. Leaving a small number of remaining mitochondrial genes. That number of genes continued to decline over time of estimated 1

billion years and it is assumed that hardly any gene transfer has happened up to this date. The highly speculated reason of that event is the assumption of a small change in the genetic code of the mitochondrial DNA, which disabled the ability of horizontal gene transfer [29].

1.3 Mitochondrial Damage, Causes and Current State of Research

Mitochondrial DNA (mtDNA) is potentially prone to accumulate mutations during the process of DNA replication and independently of replication due to oxidative damage. Evidence from 1950's suggested that mitochondrial functions are consecutively impaired by the destructive force of oxidative damage [30]. The reason that mitochondria were so important in the free radical theory of aging was, that during the 1960 and 1970's they were accounted for the main source of oxidative stress in the cell; the main source of reactive molecules, also called free radicals, which cause oxidative damage to macromolecules such as proteins, lipids and DNA [31]. Therefore, the accumulation of that damage seemed to be heavily involved in aging. This idea started the free radical theory of aging, published by Harman D. and was the first detailed mechanistic theory of aging, first published in 1956, and remained until today as foremost dogmatic pillar of how aging actually works. This has been largely discredited [31]. The main argument against this theory is, that some types of mutations are more likely to occur, depending on the mechanism by which the mutation is created. Additionally, the frequencies of different kinds of mutations can be measured by DNA sequencing. Some mutations provide no indication as to their mechanism, but the types that do are: G:C to T:A transversion, which are characteristic of ROS, and C:G → T:A and T:A → C:G transitions, which are characteristic of replication errors [30], [32], [33]. mtDNA tends to accumulate these transition mutations with age, and not the transversions, so it's concluded that ROS does not contribute to mtDNA damage with age. All those papers arguing for ROS where generally written before the results of mtDNA sequencing were known. However, there still appears to be conflicting evidence that reactive oxygen species (ROS) depicts a subset of cellular damage, which is associated with aging and affecting mitochondrial turnover rate [32], [30].

Mitochondrial turnover is a known process that prevents mitochondria DNA mutation accumulation only if it preferentially destroys mutated mitochondria. This process is mediated by mitophagy, which is essentially the autophagosomal clearance of damaged mitochondria [34]. Over time mitochondria can accumulate damage via DNA mutations and impaired protein complexes, or damaged lipid bilayers. As a response, the cell offers a set protective molecules, PINK1 a kinase and Parkin, which are the first responders to mitochondrial damage. PINK1 is basically a molecule sensor for damage and can switch on Parkin, facilitating the extension and selective binding of the autophagosome [35], [36]. Through canonical pathways the autophagosome fuses with the lysosome and the compounds are recycled by hydrolases. It is worth to notice that patients with an early onset of Parkinson's disease (autosomal recessive Parkinson's disease) showed that these two proteins play a key role in this disease, which manifests in neuronal cells [35]–[37]. 50% of autosomal recessive patients in early onset of Parkinson's disease showed a staggering proportion of mutations in Parkin and only a minor 5% have mutations in PINK1. By analyzing

the brain tissue of these patients, hallmarks of mitochondrial dysfunction such as accumulation of ROS, a defective electron transport chain and a selective loss of dopaminergic neuron cells, which leads to tremors and impaired motor function associated with Parkinson's disease (PD) [4], [34], [35]. It became clear, that mitophagy is the major mechanism to suppress the pathology in PD; hence, it is important to understand, how Parkin and PINK1 are coordinating these protective effects. Mitophagy occurs essentially in 3. Distinct steps, the initial tagging of mitochondria, recognition by the autophagy machinery, creating an autophagosome and the fusion with the lysosome, leading to the degradation of the autophagosome [4], [34], [35], [37], [38].

1.4 Cell Lines Tolerant of mtDNA Depletion

Although cellular respiration is needed to acquire energy in form of ATP by utilizing glucose and oxygen as major reactants, certain cell lines (known as rho 0 cells) are capable of proliferating without oxidative phosphorylation in culture, thereby not able to use the electron transport chain as a result of excessive deletion of the mtDNA [6], [39]–[41]. Rho 0 cells used in David M. Sabatini's Laboratory are derived from the human osteosarcoma cell line 143B, (mtDNA was depleted by ethidium bromide) and are dependent on uridine and pyruvate supplementation for growth and viability [42], [43]. Additionally, these supplements can be used as reliable selective markers, because pyruvate acts as electron acceptor for anaerobic glycolysis and uridine substitutes the compromised pyrimidine synthesis [44], [45]. Depletion of other cell lines vary in viability (fig. 1).

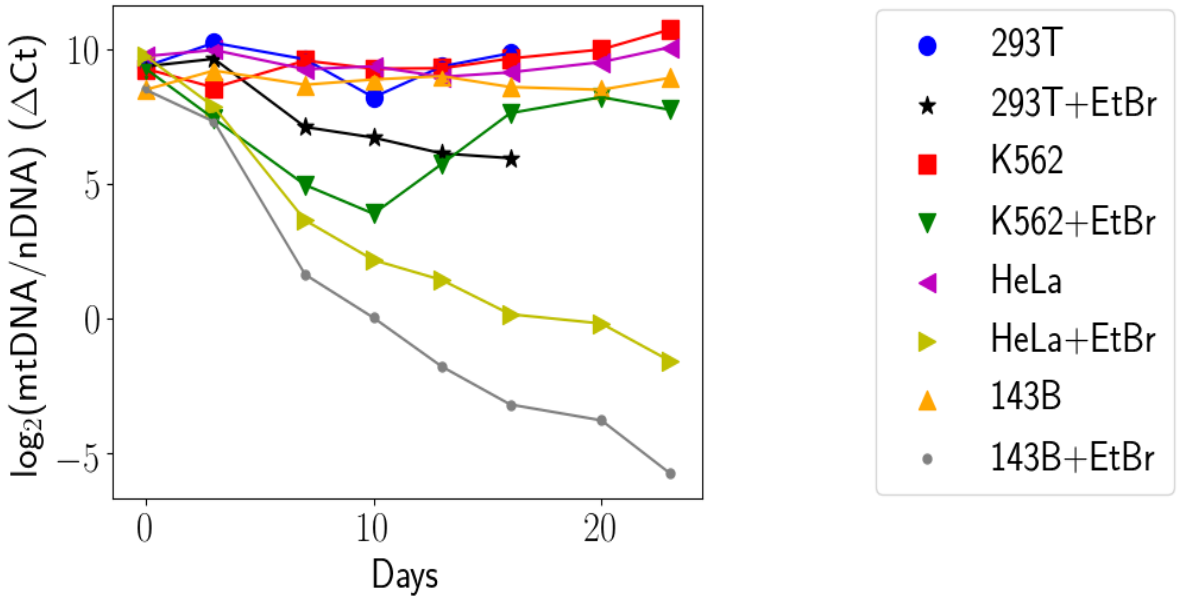

Figure 2, Mitochondrial DNA depletion via Ethidium bromide treatment. Cells were treated over a period of 25 days with 150 ng/ml EtBr. At each timepoint mtDNA and nuclear DNA (nDNA) was measured via qPCR [unpublished preliminary data].

1.4.1 Uridine Auxotrophy

Nucleotides are important biological molecules used by our cells for a variety of different reasons, we not only use nucleotides to DNA or RNA molecules, we also use them for glycogen, energy conversion and in many different types of major signaling pathways. There are two types of nucleotides, pyrimidines and purines. Our cells use two different pathways in order to synthesize *de novo* pyrimidines. The first pathway is called salvage pathway and the second is called *de novo* synthesis of pyrimidines [46]. The *de novo* synthesis starts by building the basic 6- carbon pyrimidine ring molecule and subsequently attaches sugar components to form the actual pyrimidine. This process takes place within the cytoplasm of the cell. The first 3 steps are catalyzed by the enzyme known as carbomyl phosphate synthetase and is located in the mitochondria. This enzyme catalyzes 3 distinct steps. It contains 3 different active sites and uses bicarbonate and 2 ATP molecules and glutamine to basically form carbomylphosphate. The *de novo* synthesis starts with bicarbonate, a relatively stable molecule, which energy status is being increased and made more reactive by adding ATP. This is catalyzed by carbomylphosphate synthetase and forms carboxyphosphate. This molecule has an additional negative charge which increases the reactiveness. Once carboxy phosphate is generated it obtains a glutamine molecule and hydrolyses it, resulting in glutamate and ammonia. This ammonia is used to attach it to the carboxy phosphate. The orthophosphate is substituted by the ammonia molecule and forms carbonic acid. Carbonic acid is phosphorylated by the carbomoyl phosphate containing an amino group and a highly charged component on the opposing side. This entire process is processed by carbomyl phosphate synthetase. After this step aspartate transcarbomylase attaches aspartate and forces the release of the phosphate group, resulting in the formation of carbomyl aspartate. In the next two steps, orotate the 6 membered pyrimidine ring is synthesized, enforced by a dehydration step, which releases a water molecule followed by a reduction step of NAD+ to NADH + H+ forming orotate. Once orotate is synthesized the sugar component phosphoribosyl pyrophosphate (PRPP) can be attached, mediated by the enzyme pyrimidine phosphorybosyltransferase. In this process the pyrophosphate molecule is released and orotidylate intermediate is generated. The last step is mediated by orotidylate decarboxylate, used for a decarboxylation step forming the uridine mono phosphate (UMP) molecule. UMP Kinase catalyzes it to uridinediphosphate and nucleotide diphosphate kinase to the respective nucleotide [47].

The conversion of L-Dihydro Orotate to Orotate takes place within the inner mitochondrial membrane and is mediated by dihydroorotic-acid dehydrogenase (DHODH); hence, a coupled process in order to facilitate the last steps of *de novo* pyrimidine generation. Rho 0 cells are completely depleted of mtDNA therefore not capable of respiration and subsequently depended on uridine as a supplement to bypass the previously described pathway in order to enforce *de novo* pyrimidine synthesis [47], [48].

1.4.2 Glucose Versus Galactose Metabolism in Rho 0 Cells

Galactose is a hexocarbohydrate monosaccaride and is usually metabolized by milk intake, as it is a component of lactose (consists of galactose and glucose), fruits and vegetables. Galactose is metabolized by a specific pathway called Leloir pathway. After uptake, galactose is primarily transported by the sodium depended glucose transporter 1 (SGLT1) transporter into the intestinal epithelial cell, such as glucose. Once it has been transported into the intestinal cell it will be released into the bloodstream by glut 2 transporters. After a cell took up β-D-Galactose it will converted to α-D-Galactose by galactose mutarotase. After that, α-D-Galactose is further processed by galactokinase to galactose-1-phosphate; the phosphate is obtained by ATP. Once this galactose molecule is phosphorylated the galactose is sequestered to that cell. Then galactose can be further processed by galactose-1-p-uridyltransferase, which utilizes a UDP-glucose and converts it to UDP-galactose resulting to glucose-1-phosphate [49]. UDP-galactose is usually used for proteoglycan synthesis, or lactose production (in the mammary gland). If UDP-galactose is not used, UDP-gal epimerase recycles abundant UDP-galactose and converts it back to UDP-glucose, which may be used for glycogen synthesis. Afterwards, glucose-1-phosphate is further converted to glucose-6-phosphate by phosphoglucomutase and feeds into the glycolysis pathway [48], [49]. However, if rho 0 cells are supplemented with galactose, they will ultimately die due to the fact that they cannot rely on mitochondrial ATP, because of impaired ATP synthase. This means that mtDNA depleted rho 0 cells need glucose to obtain ATP strictly from glycolysis [50]–[52].

1.5 Principles of CRISPR Multiplexing

Classical screens prior CRISPR screens were predominantly used within a forward genetics approach, where researchers mutagenized cells or organisms; then, tested on phenotypes (e.g. resistance to a drug) and finally discovered the gene, which is responsible for the phenotype. With the sequencing of the human genome, a number of different technologies arose and enabled the approach of reversed genetics [53]. This approach targets specific genes and basically observe resulting phenotypes. Techniques such as RNAi for specific gene perturbations were used to effectively endogenously incorporate chemically synthesized short RNA molecules, or a lentivirally encoded hairpin into the cell's RNAi processing machinery, causing the degradation of a target RNA molecule [54]. Furthermore, genome-scale reverse genetics started to become popular, due to its efficiency and the potential to discover all genes involved in the process of interest. This provides a much more efficient way to associate the gene with the phenotype. There are two general strategies for large scale genome screens, pooled library screening, and arrayed library screening [55]. In arrayed library screens, each well is associated with one gene knockdown, whereas in pool library screens, lentiviral transduction incorporates several CRISPR/Cas9 sgRNAs, carrying plasmids into adherent cells (favourable HEK293T). The plasmids usually already code for cas9. After transduction this pool can be subjected to selection and pooled screening. In the end, the populations are subjected to next generation sequencing and statistical analysis to screen (comparison of treated population with untreated population) for suitable hits, indicating a phenotype of interest [56]. RNAi screens are nowadays considered to be less precise, more expensive and prone to severe off-target effects compared to CRISPR

screens. The most important difference between these methods are that RNAi methods are based on knockdowns of transcription on mRNA level, whereas CRISPR technology is based on indels in genes causing functional gene deletion at the DNA level [54], [57].

Typically, pooled screens are growth-based screens, where the increase or decrease of growth of cancer cells, or the modification of a drug is observed. For example, the transcription factor activity can be observed by coupling it to a fluorescent reporter and subject them to flow cytometry-based screens, or it can be coupled to a resistance marker, (e.g. doxycycline or blasticidin) followed by viability screens reporting on the activity on the associated promoter. In case of mitochondrial based genes affecting respiration, we can use a death screen approach by utilizing pre-labelled mScarlet (red) and GFP cells, transducing the mScarlet population with the sgRNA targeting the gene of interest and screening it against untreated prelabelled GFP cells in order to compare growth in glucose versus galactose medium. If sgRNAs targeted genes associated with respiration, cells expanded in galactose must have a significantly slower growth rate compared to cells passaged in glucose. Furthermore, rho 0 cells depict an excellent control, because of their already impaired cellular respiration [58].

1.6 Multiple Guide Vectors

In order to increase the knockout efficiency, multiple guide vectors theoretically improve CRISPR screens by deleting several exons at once. gRNAs are typically expressed by pol3 promoters, or U6 promoters; hence, by using multiple U6 promoters, recombination and instability of the vector is inevitable [59]. Thus, using promoters such as, H1, sU6, can avoid recombination. Goldengate assembly facilitates a simple one step ligation process by utilizing type 2 restriction enzymes. Restriction enzymes cut DNA by creating two insertions, one in each sugar phosphate backbone. They are classified into types according to their structure and if they cut the DNA substrate at the recognition site, or down-/upstream of it. Classical type 2 restriction enzymes are commonly used in molecular cloning. Each enzyme recognizes a specific sequence, usually palindromic, and cut the DNA substrate within the recognition site leaving sticky or blunt ends. When a desired fragment of DNA is released from a plasmid using a pair of classical type 2 restriction enzymes part of the recognition sequence will be present after the cut. This offers the opportunity to be ligated to other pieces of DNA with compatible ends (usually cut with the same pair of enzymes) within a reaction mix. Golden Gate cloning uses type IIS restriction enzymes, which cleave outside their recognition sequences, leaving 5´ overhangs. After the cleaving event, there is now a sequence requirement for the identity of bases in the cleavage site. When the fragment is cut by type IIS enzyme is being released no part of the recognition sequence will be present in the released fragment. This fragment can be ligated to other fragments with the compatible sequence without the recognition sequence present [60]. For example, 5 different promoters each with a unique gRNA of interest and the associated scaffold is flanked by different BbsI recognition sites, which cuts downstream of its recognition site, producing 5’ overhangs. These overhangs have a unique compatibility to each other and the plasmid, intended for the final multiple guides. The plasmid also has BbsI sites in opposing directions, leading to the ligation of the cut DNA fragments. This method facilitates a one-step reaction, by mixing

5 previously annealed fragments with the vector, together with the type IIS restriction enzyme and a T4 ligase to complement the overhangs [61].

1.7 Aim

By utilizing CRISPR/Cas9 technology to knock out specific genes obtained from the CRISPR Screens in 143B osteosarcoma cell lines and comparing the proliferation rate to mtDNA depleted Rho 0 cells, we are able to create an excellent model to confirm and further study mtDNA associated genes. After successful confirmation of the hits, we are going to further investigate cellular respiration by conducting mitochondrial stress tests in the knockout cell lines, and additionally, observe localization of the overexpressed gene. This project aims to elucidate mechanisms affecting cellular respiration and genes required for a functional electron transport chain. Discovering novel functions of mitochondrial associated genes can lead to novel insights into the mitochondrial theory of aging and other mtDNA disorders as degenerative diseases associated with diverse mtDNA mutations Parkinson's Disease, ataxia, dysphagia, ptosis, dystonia, pancytopenia and psychiatric disorders such as schizophrenia [4], [30], [40], [62].

2 Materials and Methods

2.1 Generating Constructs

2.1.1 Multi Guide Vector and gRNAs for CRISPR Screen

In order to generate 5 different sgRNAs with each individual promoter, 5 vectors (sgOPTI Plasmid #85618 established in David M. Sabatini's Lab) with already cloned 7SK, hU6, H1, mU6 and sU6 promoter, were linearized with the enzyme BsmBI (Table 1). The same procedure was conducted by establishing constructs for the CRISPR screen validation with the exception of using the already established in-house LC2OPTI Cas9 vectors (characteristics: a blasticidin resistance box, version 1: mScarlet, version 2: neoGreen). After the incubation of 1h at 55°, 10x LI-COR orange loading dye was added to the reaction and then loaded into a 1% Agarose DNA Gel (in TAE Buffer) with 0.05 µg/mL EtBr (run at 120V for 1 hour and 30 min. at room temperature.

Components	Volume
sgOPTI/LC2OPTI plasmids	1 µg
BsmBI (NEB #R0580L)	1 µg
NEBuffer 3.1 (NEB # B7203S)	5 µL
ddH_2O	Up to 50 µL

Table 1: Sample Mix for Linearization of sgOPTI Vectors.

Afterwards, the gel was subjected to imaging with the Azure c200 gel imaging workstation to validate the correct band size (~7.1 kbp) of the linearized backbone. The correct band sizes were cut with a razorblade, transferred to a 2 mL Eppendorf tube and incubated in QG buffer (3 Volumes of Buffer to 1 Volume of gel) from QIAquick gel extraction kit of QIAGEN for 10min at 50° on a shaker for further gel extraction. Then, 1 gel volume of isopropanol was added to the sample mix, resuspended 4 times and sample mix was applied to the QIAquick spin column (the columns were placed on a vacuum manifold). QG Buffer was added again, followed by a wash with PE buffer. Then, the columns were centrifuged for 1 min at 17,000g, the flow through was discarded, and the QIAquick column was placed into a 1.5mL microcentrifuge tube. To elute DNA Buffer EB was added, incubated for 5 min at room temperature and spun down afterwards. Sample concentrations were measured via Nanodrop and used for further cloning.

Before amplifying the promoter regions and scaffold, the appropriate gRNA had to be ligated first. Oligo pairs were phosphorylated and annealed (Table 2), then the sample reaction was diluted 1:200 and used for the ligation reaction for 10 min. at room temperature. In the final step, ligated constructs were transformed into chemically competent Stbl3 bacteria and used for virus production.

Component	Volume
Oligo 1	100 µM
Oligo 2	100 µM
10x Ligation Buffer (NEB # B0201S)	1
ddH_2O	6.5 µL
T4 PNK (NEB #M0201S)	0.5 µL

Table 2: Phosphorylation and Annealing Step for gRNA generation.

Temperature	Time
37°	30 min.
95°	5 min.
95°	Ramp down to 25° at 5°/minute

Table 3: Annealing Conditions for CRISPR Oligos.

Component	Volume
BsmBI digested Plasmids (50 ng)	X µL
1:200 diluted oligo complex	1 µL
10x Ligation Buffer (NEB # B0201S)	X µL
T4 Ligase M0202M	1 µL

Table 4: Ligation of sgRNAs of Individual sgOPTI Plasmids.

Prior to transformation, kanamycin agar plates (Teknova, #L1010) were gathered from the cold room and placed in the warm room at 37°. Chemically competent cells (NEB, #C3040H) were obtained from the -80° freezer and thawed slowly on ice for about 5 min. About 5% volume of DNA samples to competent cell suspension was added to competent cells and incubated on ice for 30 min. Then, cells were heat shocked at 42° in a water bath for 40 seconds; followed by an incubation of 2 min. on ice. After that, SOC media was added and incubated with agitation at 37° for 45 min. In the meantime, agar plates were labeled, and glass bead were added. Then, recovered bacteria were dispensed onto the agar plate, shacked to spread the bacteria with the glass beads. Finally, glass beads were removed, and plates were incubated in the warm room at 30° overnight. The whole transformation procedure was executed under a Bunsen burner flame. The day after, colony PCRs were conducted by picking single colonies with a 10 µL pipet tip and transferring them to the PCR reaction tube with the pre made 2x Go*Taq* Master mix (Table 5). Validated colonies were picked and incubated overnight at 37° in LB media with ampicillin 1:1000 in a 50 mL bacterial culture tube. The following day minipreps were initiated by spinning the cultures down for 15 min at 4° and 3000g. The supernatant was removed with an aspirator and miniprep according to the QIAprep Spin Miniprep Kit protocol. Buffer P1 was added to the pellet and resuspended until it dissolved, then Buffer P2 was added and incubated for 15 min., followed by neutralization of the lysing with Buffer N3 and inverting the tubes until the blue indicator dye vanished. Afterwards, samples were spun down for 15 min at 17.000g at room temperature. The supernatant was applied to the QIAprep spin column, which was placed on the vacuum manifold; Buffer PB was added and column was 2 times washed with Buffer PE. The QIAprep column was placed into the collection tube and spun down, residual

washing buffer in the collection tube was discarded and the column was placed into a fresh 1.5 mL tube. Elution buffer (EB) was added and incubated for 5 min at room temperature. Then, the column was spun down at 10.000g for 2 min, followed by the quantification by Nanodrop. The 5 validated and prepped constructs were submitted for sequencing to QuintaraBio. After the final validation by aligning sequencing data with the plasmid in the database by using Benchling, the promoter region (with respective overhangs for golden gate cloning), gRNA and scaffold region (including overhangs) were amplified (0.44 kbp fragment) to facilitate further procedures with the golden gate assembly (Table 7, Table 8).

Compound	Volume
GoTaq Green 2x Master Mix (#M7123)	1x
Upstream primer, 10 µM	1 µM
Downstream primer, 10 µM	1 µM
DNA template (colony)	-
ddH_2O	Up to 25 µL

Table 5: Colony PCR Master Mix.

Step	Temperature	Time (min.)	Nr. of Cycles
Initial Denaturation	95°	2 :00	-
Initial Annealing	65°	00:30	36
Annealing	65°	1:00	
Extension	72°	0:30	
Final Extension	72°	1:00	-
Hold	4°	-	-

Table 6: Cycle Condition for Colony PCRs.

Compound	Volume
OneTaq (#M0480)	1.25 units/50 µL
OneTaq Buffer	1x
dNTPs (#N0447)	200 µM
Upstream primer, 10 µM	0.2 µM
Downstream primer, 10 µM	0.2 µM
DNA template (sgOPTI plasmids)	300 ng
ddH_2O	Up to 25 µL

Table 7: Reaction of the Amplification of Promoter/sgRNA/Scaffold fragment.

Step	Temperature	Time (min.)	Nr. of Cycles
Initial Denaturation	94°	00:30	-
Initial Annealing	94°	00:30	30
Annealing	56°	1:00	
Extension	68°	0:30	
Final Extension	68°	1:00	-
Hold	4°	-	-

Table 8: Cycle Conditions of sgOPTI Fragments.

After amplification of the 5 fragments, the samples were subjected to PCR purification according to the QIAquick PCR Purification Kit. 5 volume of buffer PB were added to 1 volume of the PCR sample mix (no pH indicator was used) and transferred to the QIAquick spin column. Further procedures were exactly conducted (without using QG Buffer step) according to the previously discussed QIAquick Gel Extraction Kit.

After PCR purification, fragments were quantified via Nanodrop and pooled together in a 1:1 ratio to conduct the reaction to generate overhangs with the enzyme BbsI at room temperature for 30 min. followed by inactivation at 65° for 20 min. on a thermocycler (Table 9). The golden gate assembly started after the pooled vectors and the already established linearized in-house vector (LC2OPTI, a lentiviral vector with puro resistance, linearized with BsmBI) were pooled together in order to achieve an insert:vector molar ratio of about 6:1 and incubated with the T4 DNA ligase for 15 min. at room temperature. This reaction was used for transformation, followed by colony PCRs, miniprep and successful sequencing. After sequencing plasmids were used for viral production and subsequently viral transduction in 293HEK cells. In order to identify successful cutting of each individual sgRNA, selected cells were transfected with LC2OPTI vectors carrying a sgRNA which cuts a few 100 base pairs downstream of the 5 cuts facilitated by the individual sgRNAs targeting the exon of the POLRMT gene. After the co transfection cells were harvested and gDNA extraction was conducted followed by analysis via DNA Gel electrophoresis on a 2% agarose gel to validate cut regions.

The gDNA extraction was conducted according to the QIAamp DNA mini protocol. Media of cultured cells was removed with an aspirator and cells were washed with 5 mL 0.01% trypsin. Then the cells were incubated with 0.01% trypsin until they detached. Cell suspension was transferred to a 5 mL falcon tube containing fresh RPMI + 10% IFS and 1% Penstrep. Cells were spun down for 5 min and 1000 rpm; after that, supernatant was removed, and cells were resuspended in 1x PBS. The PBS solution was transferred to a 1.5 mL tube and spun down for 5 min at 1000 rpm. PBS was removed and cells were resuspended in PBS again. Then QIAGEN protease K was added, followed by adding Buffer AL and 15 second pulse-vortexing. This solution was incubated for 10 min. at 56°, after that 100% ethanol was added and pulse vortexed for 15 seconds. The sample mix was applied to the column with a collection tube and spun for 1 minute at 6000g. Then the collection tube was changed and buffer AW1 was added, spun down for 1 minute at 6000g and the collection tube was changed again. During the last step the same procedure was repeated with buffer AW2 and DNA was finally eluted with AE into a fresh 1.5 mL tube.

Components	Volume
DNA fragments	0.5 µg
BbsI-HF (NEB #R3539L)	0.5 µg
CutSmart Buffer (NEB # B7204L)	2.5 µL
ddH_2O	up to 25 µL

Table 9: Generation of Overhangs of pooled DNA Fragments with BbsI-HF

2.1.2 Gibson Cloning of GeneT4

Gibson Assembly® cloning (#E2611L) was used to assemble GeneT4 within the vector pCW57.1 (puromycin resistance, doxycycline inducible, available on addgene.com: #41393). The 0.57 bp fragment for GeneT4 was amplified by using an already established vector carrying this gene with a 3x Flag tag as template for the PCR reaction. Reaction shown in Table 10 and Table 11 added the overhangs for the Gibson reaction, whereas the Gibson reaction mix was conducted by pooling together vector, insert (making up a total amount of 0.05 pmol) and Gibson Assembly® 2x Master Mix. The mix was incubated for 15 min. on a thermocycler at 50°. After the reaction the sample mix were used for bacterial transformation.

Step	Temperature	Time (min.)	Nr. of Cycles
Initial Denaturation	98°	2 :00	-
Initial Annealing	98°	00:30	32
Annealing	65°	1:00	
Extension	72°	0:30	
Final Extension	72°	1:00	-
Hold	4°	-	-

Table 10: Cycle Conditions for Gibson Reaction.

Compound	Volume
Q5 High Fidelity Polymerase (#M0491)	0.02 units/µL
Q5 Reaction Buffer	1x
Q5 High GC Enhancer	1x
dNTPs (#N0447)	200 µM
Upstream primer, 10 µM	0.5 µM
Downstream primer, 10 µM	0.5 µM
DNA template	300 ng
ddH_2O	Up to 50 µL

Table 11: PCR Reaction for Template Amplification of GeneT4

2.1.3 Virus Production

Virus for all experiments were produced by HEK293T cells in 6-well plates. First, cells were harvested, counted with the coulter counter, and seeded in RPMI + 10% IFS + 1% Penstrep cell culture media with a density of about 8*10^5 per well. The transfection mix for the virus class 2 assembly was prepared in serum free media (Table 12), aliquots were distributed into sterile microtubes, briefly vortexed and incubated for 15 min at room temperature. Cell culture was gently swirled to ensure even distribution and transfection mix was added to the corresponding well. After an incubation time of 16 h. media was changed, and harvest started again after 16 h. of the media change. The virus was harvested two times over an 8-hour interval and intermediate media changes. During the harvest the virus was collected in a 15 mL falcon tube spun down at 1000g for 5 min. and transferred to a cryotube, which was stored at -80 degree.

Plasmid and Virus Proportion	Ratio	DNA µg/well	µL/well
psPAX2	2	0.333	
Envelope (VSV-G)	1	0.167	
Construct	3	0.5	
PEI	-	-	3

Table 12:Transfection Mix for Virus Production

2.1.4 Transient Transfections

Transient transfections were typically conducted with a cell density of about 5*10^5 cells per well in a 6-well plate (transfection and seeding were conducted on the same day); following the same protocol such as the virus production, with about 1 µg/well of DNA per transfection mix, excluding the virus packaging compounds. Cells were incubated 12 h. with the transfection mix before media was changed. The selection process started after 12 h. of the media change and was performed until non-transfected control cells died. In case of GeneT4 and the multi-guide vector, 1 µg/mL puromycin was used for the selection process. After the selection cells were expanded in 10 cm plates and corresponding media.

2.1.5 Lentiviral Spinfections

All spinfections were performed in 6-well plates with a cell density of about 3*10^5 cells per well and 10 µg/mL polybrene in standard cell culture media. After seeding the cells, virus were thawed at room temperature, briefly mixed by pipetting up and down for 5 times and dispensed into the wells according to a series of 2-fold dilution over 5 wells and one control well without virus. After that, the 6 well plates were transferred to a swing bucket centrifuge and spun for 45 min. at 1000g and 37°. After the centrifugation step the plates were transferred to the incubator and incubated overnight. The viral media was changed after 16 h. and the selection process started. CRISPR Screen Validation cell lines were selected with blasticidin 10 µg/mL until the control well showed 100% cell death.

2.2 Western Blotting

For SDS-PAGE, premade 12% [Invitrogen, #NP0343BOX NuPAGE Bis-Tris] gels were used. Each well was loaded with 15 µl (10 µg of protein) of the protein samples and NEB™ Color Prestained Protein Standard, Broad Range (11–245 kDa) was used. The gels ran about 2 h. at 110 Volt in 1x SDS running buffer. The typical stack for protein transfer was structured as shown as in Figure 3. Before the stack was prepared the PVDF membrane was treated with 100% EtOH for 5 min. The assembled transfer sandwich was put into the transfer tank, which contained 1x transfer buffer. The transfer was conducted under 45 Volt over 2 h. at room temperature. After the transfer, the membrane was blocked for 1 hour with a 5% Milk in TBST solution at room temperature. Then, the 5% Milk solution was removed and the membrane was washed 3 times 10 min. Afterwards, the membranes were cut according to the expected protein size, they were transferred to a plastic pouch and sealed after the primary antibody in a dilution of 1:1000 was added. The membranes were incubated over night at 4°C. Next day, the primary antibody was removed, and the membrane was washed 3 times for 5 min. with TBST. The secondary antibody was added and incubated for 1 hour at room temperature. All blocking, and incubation steps with antibodies were conducted with the usage of a shaker. Prior film development, the membrane was incubated with the Pierce ECL substrate #32106 for 2 min. and transferred to a cassette. Films were developed with the X-OMAT film processor and the film was prior exposed for ~ 8min within the cassette. Then, pictures were scanned and digitalized with a Canon 8800F scanner and gray scaled via adobe photoshop (version CC 2019 (20.0.6)).

Figure 3, Western blot stack for transferring proteins onto the membrane. (abcam.com/protocols/general-western-blot-protocol, Access date: 5.20.2019)

2.3 Seahorse Assay

After viral transduction and the selection process, $5*10^4$ cells were seeded into the 96-well seahorse microplate in triplets and corresponding glucose rich, or galactose media. After incubation over night at 37° and 5% CO_2, media of each well was changed to seahorse media (Table 15). Seahorse plate with drug ports was hydrated with calibrant on the day prior the assay and kept in the warm room at 37°. At the day of the seahorse assay, cells were carefully washed 3 times with freshly prepared seahorse media (Table 14). Afterwards, media was changed to supplemented seahorse media and incubated for 45 min. at 37°. In the meantime, ports were loaded according to Table 13. Then the calibration of the machine for the assay was started and after 20 min. the plate with cells was mounted to conduct the assay.

	Compound	Stock conc. (mM)	Conc. in Port (uM)	Conc. per Well	Vol. per Port
Port A	Oligomycin	10	20	2	20
Port B	FCCP	1	10	1	22
Port C	Piericidin	5	25	2.5	25
Port C	Antimycin	50	100	10	25

Table 13: Drug Concentrations of Injection Port A, B and C for Seahorse Assay.

Supplement for Seahorse XF RPMI Medium	Concentration
Glucose	10 mM
Pyruvate	1 mM
Glutamine	2 mM

Table 14: Concentrations of Compounds for supplemented Seahorse XF RPMI medium.

Material/Device	Product Nr.
XFe96 FluxPak	#102416-100
Seahorse XF96 V3 PS Cell Culture Microplates	#101085-004
XF RPMI medium, pH 7.4	#103576-100
Oligomycin/FCCP/ Antimycin A/ Piericidin	#103708-100
Glucose	
Pyruvate	
Glutamine	

Table 15: Materials used for conducting Seahorse Assay.

2.4 Immunofluorescence Staining

Prior fixation, $3*10^4$ cells were seeded in a Corning® BioCoat Fibronectin 96-well microplate and incubated 24 h. at 37° and 5% CO_2 in standard RPMI cell culture media with 250 ng of doxycycline per well to induce target gene expression. Afterwards, cells were washed with PBS 3 times. Then, 4% formaldehyde in PBS was added in each well and incubated for 15 min. at room temperature. The solution was removed, and cells were washed for 3 times in PBS. Cells stained with COXVI were incubated with ice cold 100% methanol for 10 min. at -20°. Then the solution was removed, and the wells were washed with PBS for 3 times. After the PBS was removed cells were permeabilizated for 1 hour in 5% normal donkey serum and 0.3% Triton in PBS. After another washing step with PBS primary antibody 1:500 was added and incubated over night at 4°. Next day the antibody solution was removed, wells were washed 3 times for 5 min at room temperature and the secondary antibodies AlexaFluor 488 1:1000, AlexaFluor 546 1:1000 and Hoechst 33342 1:2500 were added incubated for 60 min. and washed afterwards 2 times for 5 min. with PBS at room temperature. Pictures were taken with a FluoView® FV1200 confocal microscope by using a 40x objective.

2.5 Flow Cytometry for CRISPR Screen Validation and Experimental Set Up

Already established prelabelled 143B and Rho 0 neoGreen cells, which were transduced in order to target AAVS1 were competed against 143B cells, which were transduced with a gRNA against a specific gene and mScarlet, in 2 conditions (Table 16). High glucose media and galactose media were selected as the 2 conditions for the competition. Rho 0 cells, transduced with the same LC2OPTI construct, were used as control and always supplemented with 200 µg/mL uridine and passaged in high glucose media.

High Glucose Media	**1x (g/L)**
Dextrose	4.5
Pyruvate	0.11
Uridine	0.2
Galactose Media	-
Galactose	4.05
Dextrose	0.45

Table 16: Media for 2 Condition CRISPR Competition Death Screen.

After selection, 143B transduced wild type mScarlet and prelabelled neoGreen 143B AAVSI cells were pooled in a 1:1 ratio with a density of 1.5*10^5 cells in 6-well plates. For each timepoint, cells were harvested, resuspended in standard cell culture media and adjusted to a concentration of ~1*10^5 cells/mL in a 5 mL glass tube. Cell suspension were subjected to the flow cytometer, where 5000 events per cell line were recorded. The raw data was computed by the FlowJo software (Version v10.6.1), AAVI transduced neoGreen cells and 143B mScarlet knockout cells were plotted against each other.

3 Results

3.1 Generation of a 5 guide CRISPR/Cas9 Vector

The advantage of our approach is the use of multiple guides simultaneously targeting POLRMT in order to increase the percentage of cells harbouring a mutation in the respective gene. The population of POLRMT knockdown cells can then be split between different treatments; for example, different media conditions in which mtDNA may be more or less essential. Figure 4 shows confirmation of each gRNA used to generate the 5 guide CRISPR/Cas9 vectors. Each vector carried 1 gRNA targeting a specific region within exon 1 of the mitochondrial polymerase (POLRMT). By co-transfecting these constructs with a CRISPR vector cutting several 100 bp downstream of exon 1, a secondary band should be generated. The POLRMT excision check was conducted after amplifying a 884 bp fragment from the gDNA extraction of the co-transfections (Figure 4); revealing functional gRNAs by indicating secondary bands due to the base excision repair mechanism. Lane 1 to 5 are the gRNAs targeting different regions of exon 1 and are under regulation of individual promoters; lane 6 shows the confirmation indicating the cut downstream of the exon 1 knockouts. Further sequencing showed the successfully established generation of the multi guide vector.

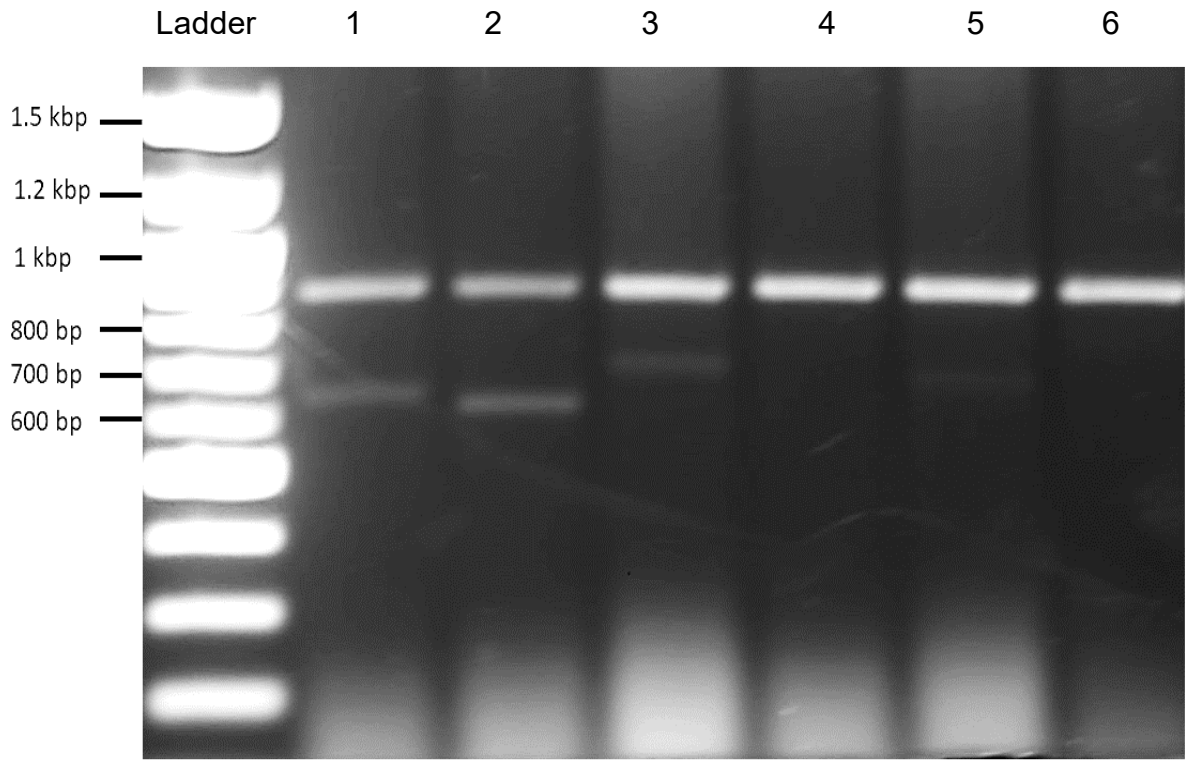

Figure 4, 2% DNA Agarose Gel of POLRMT Excision repair validation. First band of each lane is at ~900bp. In lane 1 a 650bp product can be observed; 2nd lane ~630 bp, 3rd lane ~750 bp, 4th no visible band; 5th lane indicated a ~700 bp lane and the 6th showed no secondary band as expected. The sum of each amplicon is 884 bp long, whereas the 1st lane should exhibit a 237 bp, 2nd a 262 bp, 3rd a 180 bp, the 4th 215 bp and 5th a 207 bp excision.

3.2 CRISPR Screen Validation by Using a FACS - Based Competition Assay

The FACS based competition assay is an efficient and fast paced method to screen for sgRNAs, providing insight into suitable knockout candidates within a cell population; therefore, identifying genes associated with proliferation and viability, which provides a functional selection system of screening for suitable sgRNAs. Genome-wide CRISPR screens help to understand the effects of individually knocking out the nearly 20 thousand human genes of a phenotype of interest and observe their functions in different cell culture settings, such as growth in different media conditions. As so many phenotypes are being measured, the data may contain false positives (genes that appear to be important for the phenotype but actually are not). Therefore, the first follow-up to a screen is typically repeating the same measurement on a smaller scale (i.e. validation). Indeed, we found that one gene of 5 identified in the screen (CFL1) was a false positive, whereas another GeneX6 was a true hit. We performed our validations using FACS based competition assays.

In our case these candidates are suspected to impair the mitochondrial oxidative phosphorylation system (OXPHOS). Our assay is based on the fact that OXPHOS deficient cells are still viable in medium supplemented with glucose, whereas cells supplemented with galactose are not viable after a certain number of passages. Figure 2 shows pre-labelled neonGreen and mScarlet cells pooled together with the transduced sgRNA labelled with the opposite colour. 143B Rho 0 cells were utilized as negative control, as they lack the ability to perform oxidative phosphorylation. Rho 0 cells were passaged in dextrose rich media, supplemented with uridine in order to provide proliferation and growth without constrains. Furthermore, 143B wild type cells were passaged and competed within 2 conditions; first condition was dextrose rich media; the other subset of 143B wild type cells transduced with respective sgRNA where incubated in galactose media. Before measuring the 1st timepoint the labelled mScarlet cell lines transduced with corresponding mScarlet sgRNA were mixed 1:1 with neonGreen sgAAVS1 in order to compete with each other in terms of growth and proliferation. sgRNA_2 of GeneX6 does not appear to have any effect, because the 143B wild type cell line in dextrose showed a similar positive growth rate as the wild type cell line incubated in galactose. Interestingly, sgRNA_6 and sgRNA_7 showed a rapid decline in growth in galactose media, whereas cells in dextrose media were still viable, which confirms effectivity of corresponding knockouts and suggests impaired OXPHOS. Rho 0 cells of all subset sgRNAs showed a decline in growth rate as well. Following seahorse assays (Figure 8 and Figure 9) and gene addback experiments proved the observed effect obtained by the FACS based growth assay.

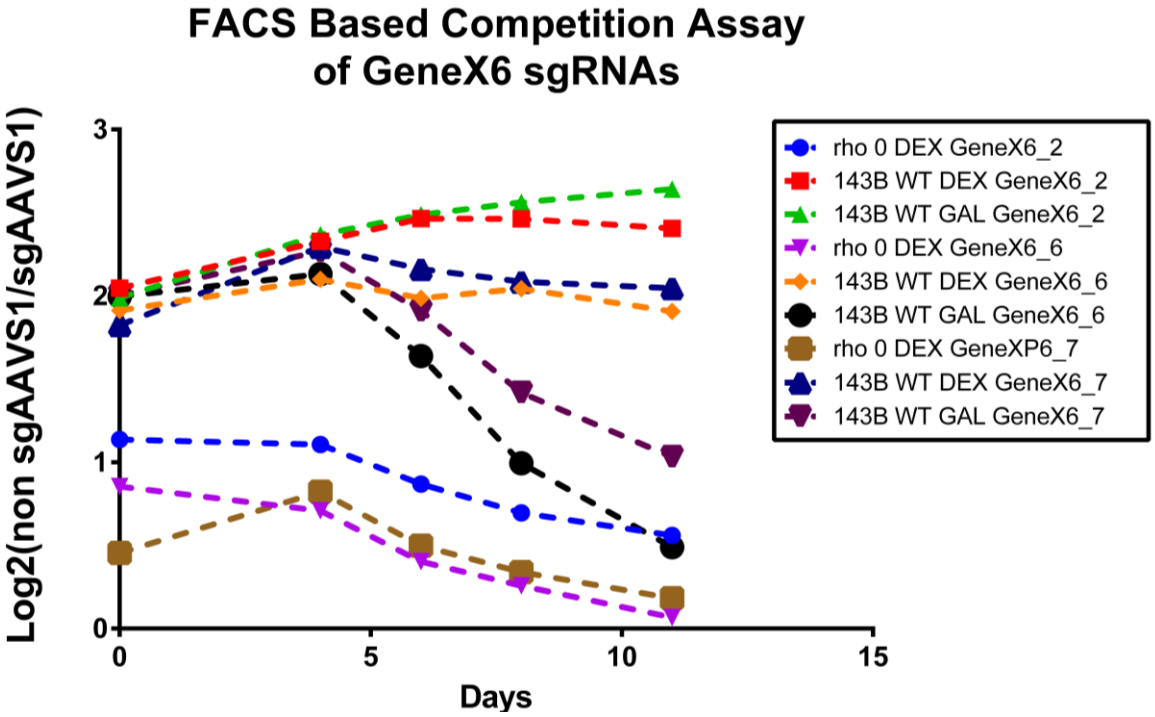

Figure 5, FACS Based Competition Assay of GeneX6. Transduced sgRNAs for GeneX6 screened against neutral control in 143B wild-type and 143B rho0 cells were screened via FACS on 5 timepoints over 12 days. Each polyclonal cell line competed with the opposite color of the same cell type (mScarlet versus neoGreen).

The same procedure was conducted with CFL1 (Figure 6) and showed an insignificant decline of proliferation in all knockouts after 5 days, leading to the exclusion of CFL1 for further experiments.

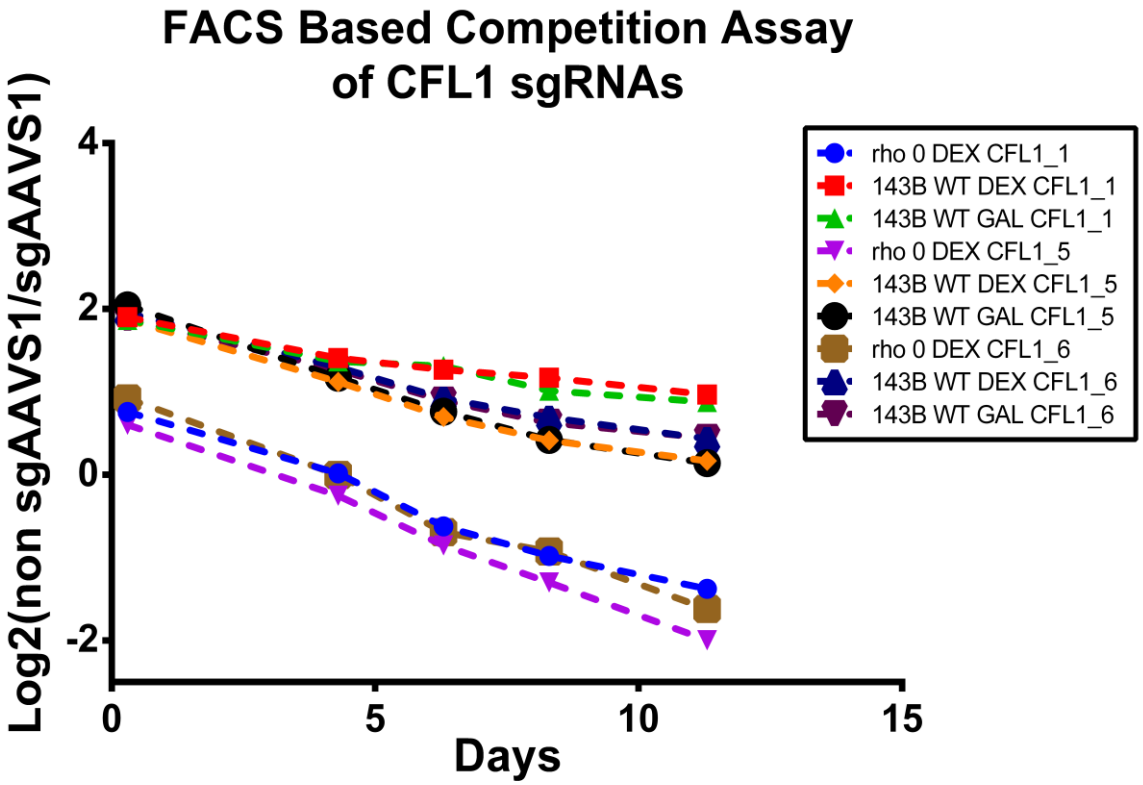

Figure 6, FACS Based Competition Assay of CFL1. Transduced sgRNAs for CFL1 screened against neutral control in 143B wild-type and 143B rho0 cells were screened via FACS on 5 timepoints over 12 days. Each polyclonal cell line competed with the opposite color of the same cell type (mScarlet versus neoGreen).

GeneY (Figure 7) showed a decline in proliferation within every sgRNA population indicating that this knockout can be associated with viability. Due to the nature of the gene, which cannot be discussed in this thesis (NDA), we identified a novel yet unknown secondary function. This protein in particular is expected to only function in respiration according to the CRISPR screen but found that it is still essential when respiration is dispensable.

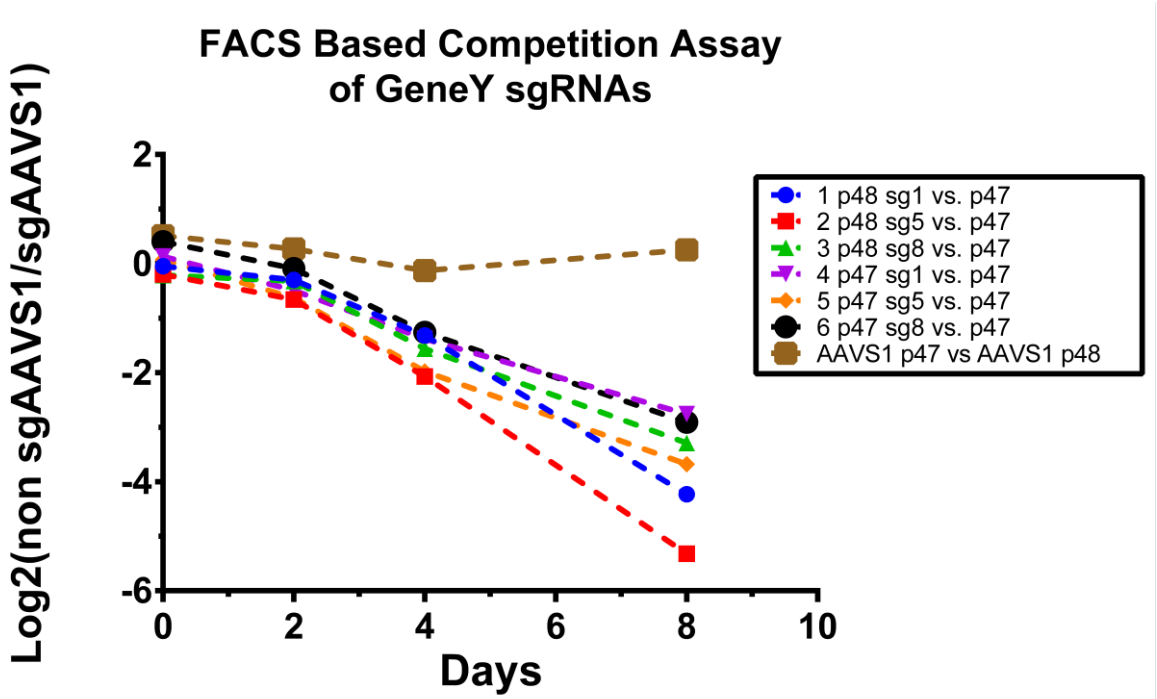

Figure 7, FACS Based Competition Assay of GeneY. Transduced sgRNAs for GeneY screened against neutral control in 143B wild-type and 143B rho0 cells were screened via FACS on 5 timepoints over 12 days. Each polyclonal cell line competed with the opposite color of the same cell type (mScarlet versus neoGreen).

3.2.1 GeneX6 Seahorse Assay

To validate the results of the FACS based growth assay (Figure 5), we established 4 polyclonal knockout cell lines targeting the GeneX6 in 143B wild type cells. These knockouts were generated by the same virus but were distinguished by different titers of corresponding viral stocks, leading to 4 knockout cell lines with different multiplicity of infection (MOI) rates. We performed 2 gene addbacks for each knockout cell line, with 2 different virus batches (cDNA 3 and cDNA 5) and expanded the gene addbacks in DMEM + galactose media, whereas the pure knockouts were passaged in RPMI + glucose media. Each individual knockout and knockout with gene addbacks underwent a mitochondrial stress test via seahorse assay (Figure 8). It is also known as live-cell metabolic phenotyping assay. This assay measures the energy producing function of each cell in real time, whether cells using glycolysis (proton efflux rate), or mitochondrial respiration (oxygen consumption rate) as a source of energy. Since we know that our targets are associated with the OXPHOS, we conducted a mitochondrial stress test in order to elucidate the oxygen consumption rate (OCR) of the knockouts and gene addback cultures in real time by exposing them to 3 well defined metabolic modulators. Oligomycin which blocks the F0 unit of the ATPase synthase and therefore blocks the proton flow leading to an accumulation of protons in the intermembrane of the mitochondria and ultimately effects the flow of protons from the matrix mediated by complex I, III and IV into the intermembrane space, leading to decreased ATP synthesis and oxygen consumption. The effect of oligomycin as inhibitor can be observed in figure 8 after 20 min., where the OCR of 143B wild type and knockouts + gene addbacks drastically decreases (20 min. after injection). After the mitochondrial hyperpolarization mediated by oligomycin, FCCP was added in order to uncouple oxidation from

phosphorylation by acting as a chemically generated artificial pore in the mitochondrial inner membrane and allows a free flow of accumulated protons; thus, leading to depolarization. This decreases ATP levels and increases ADP, which feeds into the TCA cycle. Due to the massive proton backflow, NADH and FADH is produced faster in order to mediate proton flow to the inner mitochondrial membrane without producing ATP. Therefore, increases oxygen consumption and decreasing NADH/NAD and FADH/FAD ratios, this enforces a subsequent increase of the respiratory rate. The increase of O2 consumption can be observed at the 40 min. mark. After 60 min. the inhibitors antimycin A (complex III inhibitor) and piericidin (complex I inhibitor) increases the NADH/NAD ratio, decreases the oxygen consumption, which can be observed by a rapid decline of OCR starting at 60 min. and resulting as a flat line at the ~65 min. mark. Figure 8 shows 2 KO clones with the respective rescues and the controls, whereby Figure 9 shows the basal respiratory capacity, which represents the oxygen consumption under baseline conditions of all conducted KOs and rescues.

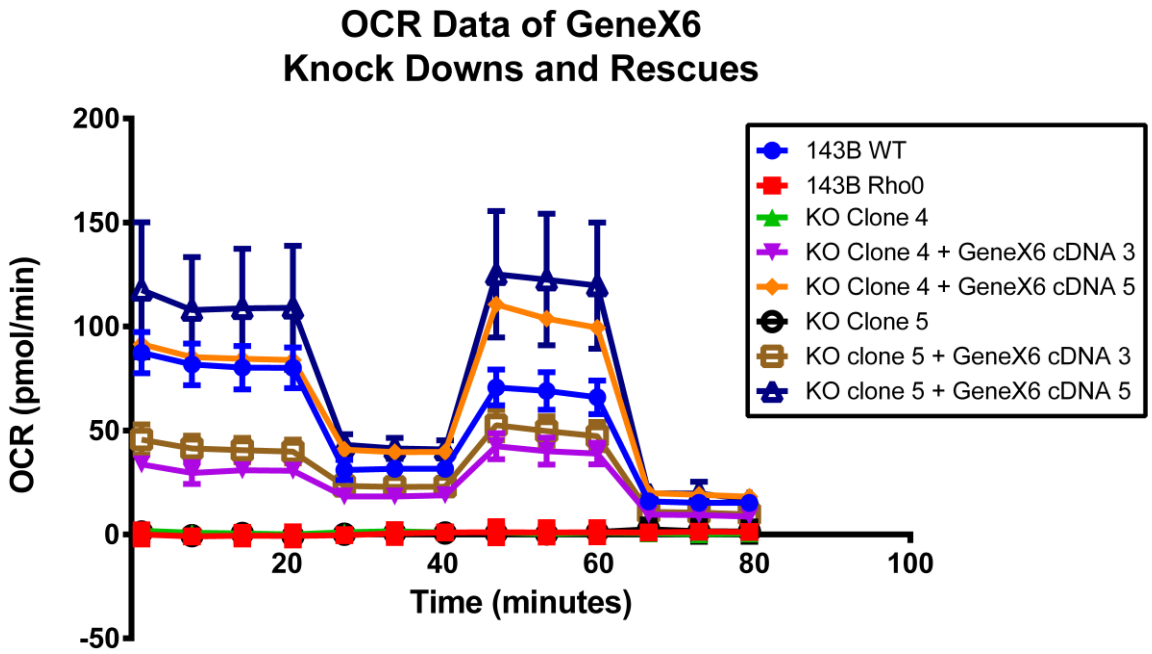

Figure 8, Seahorse Data of GeneX6 Knock Downs and Rescues. The OCR Chart shows the 2 strongest of the 4 conducted knockdowns and gene addbacks (rescues). 143B Rho0 cells are the negative control, as they lack of functioning cellular respiration, 143B wild type act as positive control to show functional respiration.

That principle works only in cell capable of using the OXPHOS, we used 143B wild type cells (blue line) as positive control and rho 0 cells (red line) as negative. Rho 0 do not exhibit oxidative phosphorylation. Therefore, we can observe a flat line, indicating a significant OCR. If our gene of interests is associated with OXPHOS, we estimated a similar behaviour, as the one we could confirm. All knockouts lack of using the OXPHOS and show a limited OCR (flat line in Figure 8, low basal respiratory capacity in Figure 9). Knockouts transduced with the gene of interest showed a successful rescue of the phenotype, which can be observed in Figure 8 and Figure 9.

The strongest achieved rescue seems to be mediated by the cDNA 5 gene addback, indicated by an OCR of about 70 to 100 (pmol/min) capable of rescuing KO 4, KO 5 and KO

8. The KO 4 treated with cDNA 3 rescued as well as the gene addback cDNA 5, the strongest observed rescue can be observed in the KO 8 rescued with cDNA 5. Taken together, our results suggest a novel function for a novel yet unknown function in our gene of interest within the mitochondria, which seems to play an important part in respiration. Furthermore, western blots (Figure 10, Figure 11 and Figure 12) prove the significant relationship within the OXPHOS.

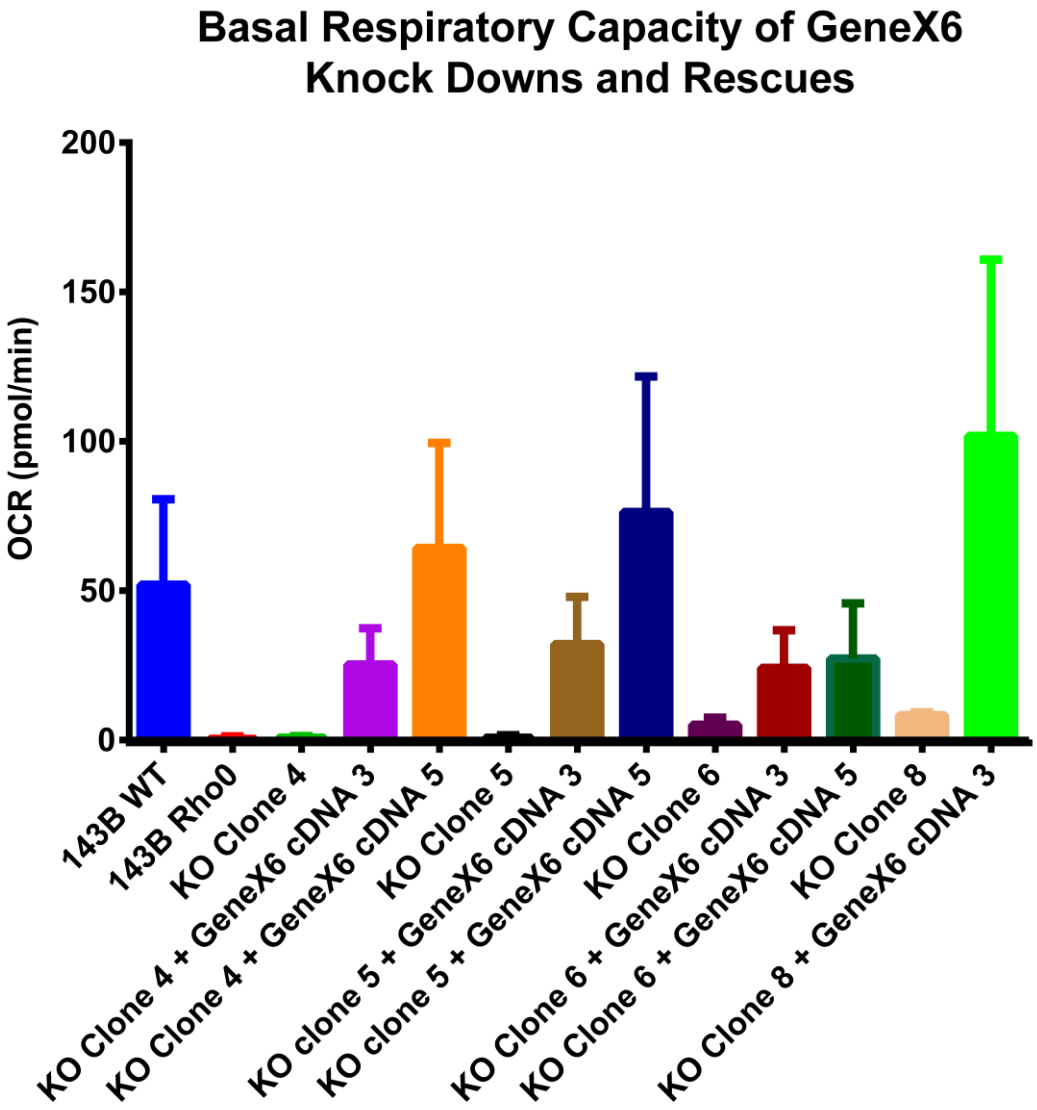

Figure 9, Seahorse Data of GeneX6, Bar Chart. The chart shows the basal respiratory capacity of knock downs and corresponding rescues.

3.2.2 GeneX6 Western Blots

Figure 10 shows the successfully established knockouts and gene addbacks by probing with MTCO2; numbers 4, 5, 6 and 8 reflect the 4 different GeneX6 knockout cell lines. Pure knockouts showed a lack of cytochrome c-oxidase gene 2 (MTCO2) expression, whereas the gene addbacks clearly rescued the knockouts shown by clear distinct bands at about ~17 kDa. Vinculin was used as a loading control. Unfortunately, the 143B wild type control failed to be probed with MTCO2 to a major extent (indicated by a small dot), rho 0 cell line showed no MTCO2 activity at all, which was expected, because of the lack of OXPHOS. The gene addback c3 and c5 seem to work equally well according to the blot. This blot underlines the role of the gene in respiration, because MTCO2 catalyses the reduction of oxygen molecules to water. Hence, the oxidoreductase activity combined with its cytochrome-c oxidase activity depicts a crucial role in performing electron transfer and is formed by subunit 1, 2 and 3 as functional core.

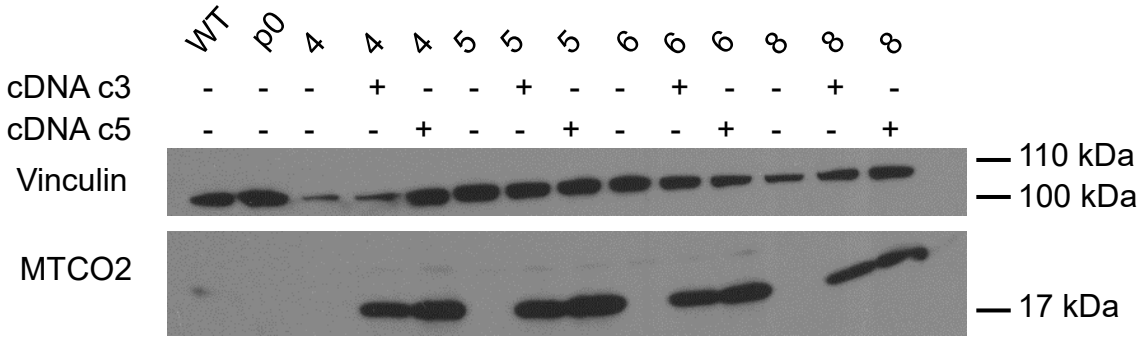

Figure 10, 1st Western blot of GeneX6 Knockouts and Gene Addbacks. 4 knockout cell lines were rescued with either gene addback c3, or gene addback c4. Samples were run on a 12% gel, probed with vinculin as loading control at ~105 kDa and cytochrome c oxidase subunit 2 (MTCO2) in order to evaluate successfully established gene addback cell lines. 143B wildtype was used as a positive control and 143B p0 cells were used as negative control.

Further investigations also showed a clear relation of mitochondrially encoded ATP synthase membrane subunit 6 (MT-ATP6) at ~17 kDa with our gene of interest. The knockouts lacked MT-ATP6, whereas both gene addback versions rescued its function. 143B WT was used as positive control and rho 0 as negative control. Knockouts number 4 with the gene addbacks were not as strongly expressed as the knockout 5, 6 and 8 rescues. Vinculin was used as loading control and indicated a slightly higher amount of protein in the knockouts 5, 6, 8 and the respective gene addbacks compared to 143B wild type and rho 0. The lack of MT-ATP6 showed an impaired proton transmembrane transporter and impaired ATPase activity, which explains the absent OCR of the previously shown seahorse assay.

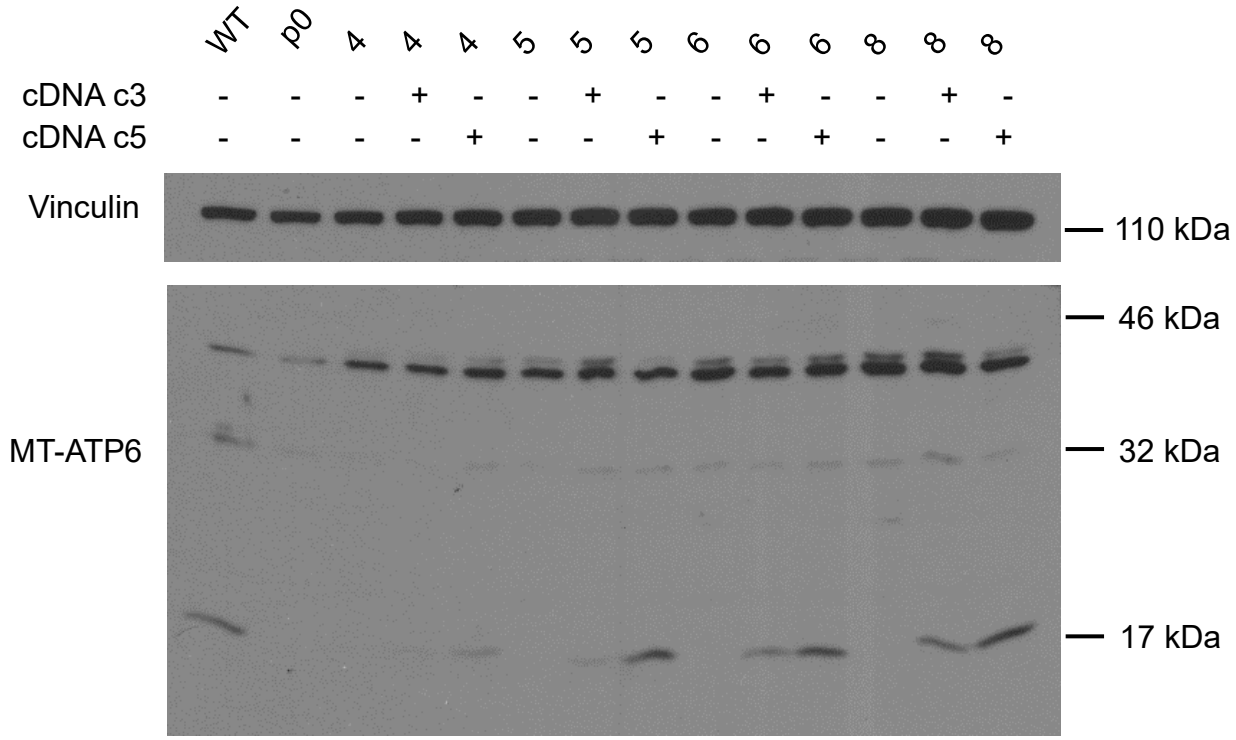

Figure 11, 2nd Western blot of GeneX6 Knockouts and Gene Addbacks. 4 knockout cell lines were rescued with either gene addback c3, or gene addback c4 Samples were run on a 12% gel, probed with vinculin as loading control at ~ 110 kDa and MT-ATP6 at about 17kDa in order to evaluate successfully established gene addback cell lines. 143B wildtype is used as a positive control and 143B p0 cells are used as negative control. Additional bands at ~32 kDa and ~43 kDa are a result of unspecific binding.

Figure 12 shows GeneX6 knockouts and gene addbacks probed with the rodent OXPHOS antibody cocktail. This antibody cocktail probes for nuclear and mitochondrial encoded proteins, which makes up important components of the OXPHOS. ATP5A, also known as ATP5F1A, is a gene coding for mitochondrial ATP synthase F1 subunit alpha and located on chromosome 18 in position 21. A lack of ATP5A is associated with mitochondrial disorder called oxidative phosphorylation deficiency 22; Nevertheless, the gene was not affected by the knockouts and it was clearly expressed in every single sample at ~58kDa. UQCRC2 coding for the mitochondrial cytochrome b-c1 complex subunit 2 (nuclear encoded) and constitutes a part of the ubiquinol cytochrome c reductase, which consists of the mitochondrial encoded gene MTCYTB and ten nuclear encoded genes; we could observe adequate expression within every sample at about ~48 kDa. The 3rd probed protein, MT-

CO1, showed only faint bands in the gene addbacks at about 36 kDa. MT-CO1 is mitochondrially encoded and codes for cytochrome c oxidase subunit 2. Typically, we would expect this protein expressed in the 143B wild type cells, but this was not the case due to lower protein loading of the SDS-PAGE gel, indicated by the loading control vinculin. The 4th protein probed by the OXPHOS rodent antibody cocktail is SDHB, another nuclear encoded protein, coding for succinate dehydrogenase complex iron sulfur subunit B and can be observed in every single sample. The expression seemed to be affected by the gene addbacks, because 143B wild type, rho 0 and pure knockouts showed faint bands at ~27 kDa, whereas the gene addbacks resulted in strong expression of SDHB. Furthermore, NDUFB8 (nuclear encoded) shows low protein expression in the gene addbacks of knockout 4, 5 and 6. The protein expression was not detected in wild type and knockout 8 gene addbacks, which might be the case due to lower protein load.

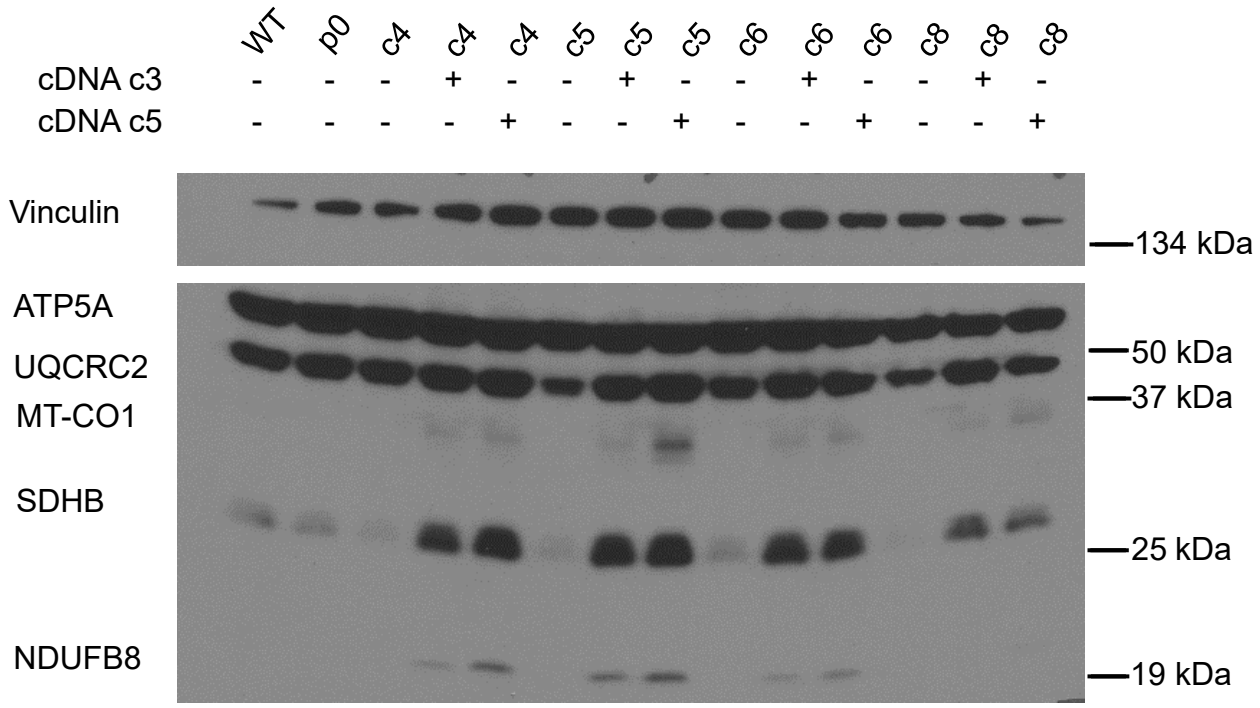

Figure 12, 3rd Western blot of GeneX6 Knockouts and Gene Addbacks. 4 knockout cell lines were rescued with either gene addback c3, or addback c4 Samples were run on a 12% gel, probed with vinculin as loading control at ~105 kDa and cytochrome c oxidase subunit 2 (mtco2) in order to evaluate successfully established addback cell lines. 143B wildtype is used as a positive control and 143B p0 cells are used as negative control.

The disappearance of several mitochondrially-encoded proteins upon GeneX6 knock-out implies that we discovered a novel function of the gene, which may be required for mitochondrial translation. We observed absence of respiration, while mtDNA levels are normally expressed in the knockout, which indicates that DNA replication and transcription are functioning. The central dogma (replication, transcription, translation) for the mitochondrial genome is a single pathway for all mitochondrial encoded genes. This means that there is one DNA polymerase, one RNA polymerase, which mostly produces a single long transcript, one ribosome and the circular DNA. Therefore, gene expression in the mitochondria is expected to be working for all the genes or none of the genes.

3.3 GeneT4 Immunostaining

The Gene T4 is a gene identified as being involved in mitochondrial function by the screen and co-essentiality analysis. Efforts to generate knockouts have failed in prior experiments due to instability of dox-on expression. Therefore, we decided to conduct immunofluorescence staining in order to observe possible co-localization within the mitochondria. COX IV, often used as mitochondrial loading control, was used to probe for cytochrome c oxidase (Complex IV) revealing the mitochondrial intermembrane (green). The gene of interest T4 was tagged by the 3x FLAG antibody (red) and the nucleus was stained with Hoechst 33342. We subjected the samples to confocal microscopy and recorded a Z-series with a magnification of 40x. The staining shows co-localization of COX IV and our protein of interest, proving that it must exhibit an unknown function and proves the relationship to mitochondria suggested by the co-essential screen.

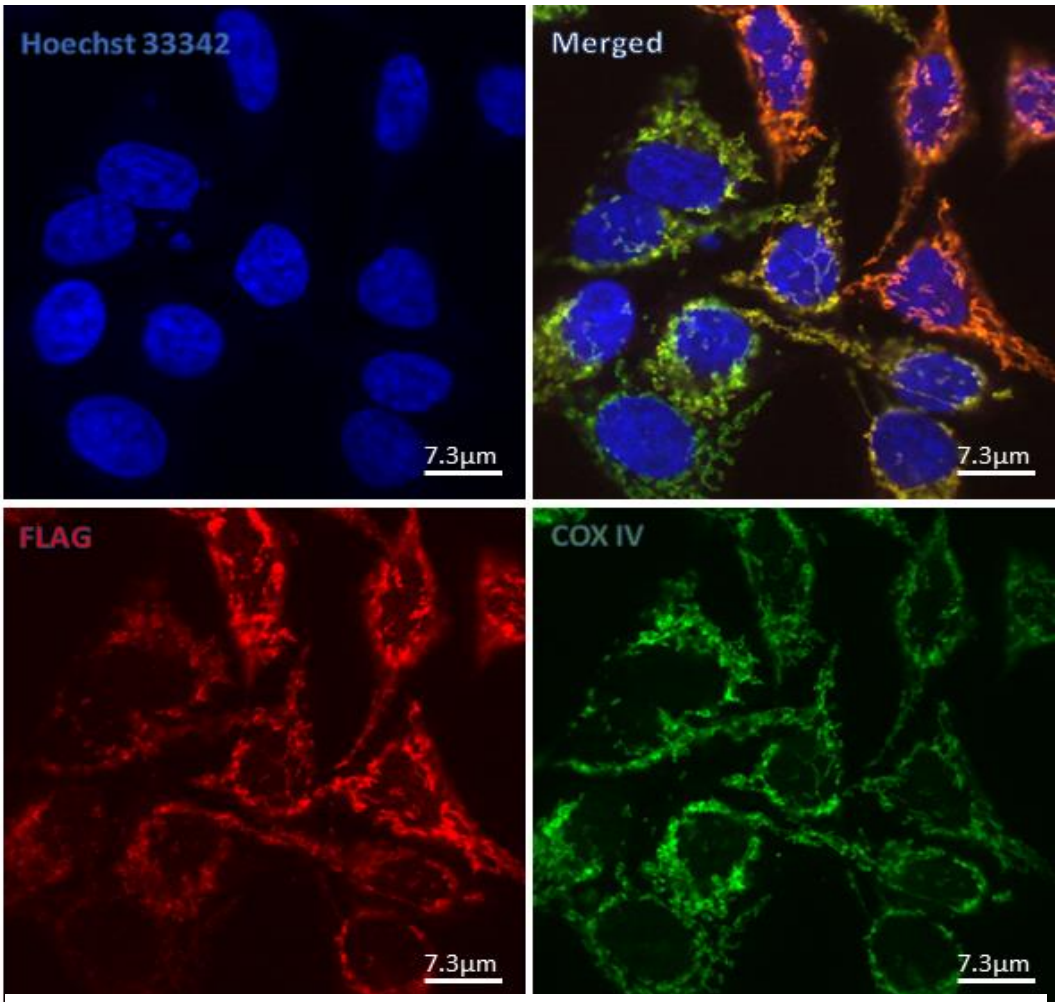

Figure 13, Immunostaining of transiently transfected HeLa cells. Cells were incubated with doxycycline approx.12 h. prior fixation and processed as described in the protocol. Localization of the gene of interest was detected with AlexaFluor® 568 co-localizing with cytochrome c subunit 4 (COX IV), a terminal complex of the electron transfer chain. COX IV was detected with AlexaFluor® 488 and the nuclear staining conducted with Hoechst 33342. Pictures were taken via confocal microscopy at a magnification of 40x.

4 Discussion

The project addressed two main questions: What is the significance of genes CFL1, GeneX6 and GeneT4 for respiration and why do some cell lines exhibit greater tolerance for mtDNA depletion than others? All of these genes were identified from prior genome-wide CRISPR screens [58]. We found that CFL1 is not related to respiration, while GeneX6 plays a critical role in mitochondrial protein synthesis. The role of gene T4 remains to be determined but we showed that it does localize to mitochondria. For this, our efforts focused on developing more efficient methods of depleting mtDNA. The context and implications of these results and efforts are discussed in more detail below.

4.1 Future Studies of GeneT4, GeneX6 and GeneY

Mitochondria are generally seen as the main source for bioenergetics, but they also respond to physiological processes. If a cell encounters a physiological signal because of inflammation, cellular differentiation signals, growth signal response, or a T-cell response to an antigen, the mitochondrial response is not only integrated by underlying signalling pathways, which eventually into a gene transcription factor network, or chromatin remodelling process; mitochondrial determent cell fate processes due to internal assessment of mitochondrial fitness [15], [63]. Hence, mitochondria are signalling organelles by itself, which can be observed by the examples of NF-κB signalling, α-HIF, NOD-signalling and every epigenetic principle, which uses metabolites derived from mitochondria, such as acetyl-CoA, α-ketoglutarate, or succinate [26], [63]–[66]. We focused our work on several genes, which revealed new players within cellular respiration and reported a novel function affecting OXPHOS. GeneX6 is required for mitochondrial translation, but its exact role is not known yet. Future work will include immunoprecipitation and mass spectrometry to elucidate protein-protein interactions. GeneT4 did not exhibit a specific phenotype yet, but this will be further studied by metabolite profiling on knockouts versus gene addbacks, similar to experiments conducted with GeneX6, to look for perturbation of mitochondrial metabolism. Likewise, the confirmed hit, GeneY, is a newly discovered mitochondrial protein required for viability in absence of respiration, but its function independent of respiration is yet unknown.

4.2 Advantages and Disadvantages of the Multi-Guide-Vector Approach

A five guide (multi-sgRNA) construct, which is able to target multiple exons within the same gene, depicts a useful tool for efficient knockouts. By delivering multiple sgRNAs at once in combination with a lentiviral expression system, we are able to offer constitutive multi targeting in an elegant way, which may facilitate an advantage in mini CRISPR library screens and knock downs of a spectrum of interconnected genes [59]. Additionally, several papers already proved that this approach achieves a significantly higher knockout efficiency in polyclonal cell lines [67]. We successfully developed construct but still need to verify the efficiency by comparing the knockout efficiency with co-transfections. A downside of utilizing a multi-sgRNA vector approach is that the construct may be prone to recombination during

virus production, which has to be monitored in future experiments. Moreover, off-target effects still remain a challenge; however, there are already several ways to counter these unwanted effects. For example, utilizing novel and state of the art algorithms to avoid potential off-targets (Cas-OFFinder, Crispor) by considering that following properties play a key role in specificity and avoiding of off-target effects; identity of complement base pairs, their position within the gene, the whole sequence composition in general and overall locus sequence [57], [68], [69]. Another beneficial modulation is the titration of expressed SpCas9, which is able to refine cleavage events between off-targets and on-targets. This can be utilized via degron tagged SpCas9, activated by specific nontoxic ligands. A degron constitutes a peptide domain, typically mediating protein degradation, and is mainly used as recognition motif to increase the rate of how the ubiquitin system operates for further protein degradation. Degrons can be fused with SpCas9 to actively control cas9 expression via ligand binding, which avoids overexpression and hence reduces possible off-target effects [70], [71].

4.3 Multiple Ways of Generating Rho 0 Cell Lines

Once the multi-sgRNA guide approach has been verified as a robust tool for CRISPR/Cas9 mediated knockouts, it can be used to efficiently knock out multiple mitochondrial genes simultaneously; thus, generating rho 0 phenotypes in various cell lines, which can be further studied in order to connect mitochondrial associated diseases to corresponding mitochondrially encoded genes. Generating rho0 cells is typically achieved by EtBr treatment but this method has been shown to be unreliable [72]. The main disadvantage of using this method are mutagenic side effects on nuclear DNA loci due to the long exposure to EtBr (rho 0 phenotypes start to manifest after about 10 Days (Figure 2) [43]. Another approach to eliminate mitochondrial DNA without disrupting nuclear DNA is the utilization of restriction enzymes. It appears that the mitochondrial overexpression of the Y147A mutant uracil-N-glycosylase and overexpression of bacterial Exonuclease III in a transient transfection set-up with plasmids pMA4008 (available on addgene.com: #70109) and pMA3790 (available on addgene.com: #70110) lead to rhofication of several kinds of cell lines. By introducing these novel approaches, Alexeyev *et al* demonstrated an efficient and fast method to induce rho 0 cells, without exposure of mutagenic compounds and proved its robustness by generating rho 0 cells in mouse, rat and human cell lines [72], [73].

4.4 Mitochondrial Replacement Therapy and the Importance of Studying mtDNA Diseases

The majority class of mitochondrial mutations occurs in the maternal lineage passing on maternal inheritance diseases (12s rRNA, 16s tRNA, ND1, ND2, ND3, ND4, ND5 and ND6 coding for complex I, cyt b coding for complex 3, CO1, CO3 for complex 4 and ATPase 6 for complex 5). A mutation in the 12s rRNA at position A1555 is known to initiated sudden deafness in midlife [74]. Another gene mutation at position A3243 in the tRNA leucine gene gives rise to diabetes at a 30% mutation rate, whereas a 50% mutation rate of the same gene cause neural muscular disease [75]. Mutations at the tRNA glutamine gene T4336 predispose the patient to Alzheimer's and Parkinson's disease [1], [30], [76].

Our project and similar studies of mitochondria related genes are paving the way to an emerging topic; Mitochondrial replacement therapy (MRT), also called three parent reproduction technique. This method is used to prevent mitochondrial related diseases transmitted by the maternal carrier. The prospective technology of MRT techniques is destined to prevent the transmission of mtDNA diseases to the child and is going to be slowly integrated as new reproductive technology in several countries all over the world. Statistically, the prevalence in the working age population of such genetically transmitted diseases are about 1 in 10000 people and 1 in 200 people carries a pathogenic mtDNA mutation, which states an emerging clinical concern [77].

There are two methods to facilitate MRT, mitochondrial spindle transfer, and pro-nucleus transfer. Mitochondria are evenly distributed in the oocyte surrounding the nuclear genome. By transferring the nuclear genome into a donor oocyte with genetically healthy mitochondria and without the nuclear genome of the donor, followed by the in vitro fertilization an embryo with normal mitochondria can be generated. This procedure is called the mitochondrial spindle transfer. In principle there are no major changes, for the patients, compared to a standard in vitro fertilization. First, the egg is recruited, and the egg is harvested. After that donor oocytes are screened for healthy mitochondria and mitochondrial replacement takes place. Then, *in vitro* fertilization takes place followed by embryo growth, an embryo biopsy and embryo freezing. Several studies have shown that these manipulations are safe and that mitochondrial carry over was below 0.5%, suggesting an effective strategy at preventing mitochondrial diseases without direct modification of the DNA and altering inheritance of nuclear alleles that determine physical features. A similar technique called nuclear transfer differs at the starting point where the karyoplast containing the parents' pronuclei from a first day zygote is transferred to a donor oocyte, whereas the pronucleus of the donor was discarded beforehand [77]. The world's first parent IVF was carried out in Mexico by US scientists in 2015 and doctors in the United Kingdom were granted permission by regulators to carry out this method in 2018. This method offers a solution for parents who desire offspring which share a nuclear genetic connection with them, and which are carrier of mtDNA diseases, facing the prospect of giving birth to children of profound and even fatal complications. Thus, MRT facilitates the only safe reproductive option for mitigating maternal transmission of mtDNA in children and preserve the genetic connection and relationship of prospective parents with their child [77], [78]. Furthermore, it is also eradicating further mtDNA diseases of future descendants. Mitochondrial diseases are genetically heterogenic and each of about 145 genes causes a monogenic disease, if disrupted. Only 13 proteins cause mtDNA related diseases in 15-20% of paediatric diseases, which are maternally inherited. The main challenges are finding new phenotypes for established genes, new genes in OXPHOS pathways and interpreting pathogenic coding and non-coding variants [79].

Today it is common knowledge that mitochondria control a variety of physiological responses and are perturbed in various diseases. Nevertheless, common diseases were primarily approached from an anatomical and mendelian perspective, but the role of bioenergics and non-mendelian bioenergic inheritance has been largely ignored over decades. All major

metabolic-, visceral-, heart-muscle diseases, neuropsychiatric disorders, cancer and aging are still unsolved and not fully understood [14], [21], [80]–[82].

Further studies of mtDNA depletion will provide better understanding of physiological consequences of respirational defects like those occurring in human diseases (especially in children) and aging.

5 Bibliography

[1] N. A. Khan, P. Govindaraj, A. K. Meena, and K. Thangaraj, “Mitochondrial disorders: challenges in diagnosis & treatment.,” *Indian J. Med. Res.*, vol. 141, no. 1, pp. 13–26, Jan. 2015.

[2] V. F. Gonçalves *et al.*, “A Comprehensive Analysis of Nuclear-Encoded Mitochondrial Genes in Schizophrenia,” *Biol. Psychiatry*, vol. 83, no. 9, pp. 780–789, May 2018.

[3] K.-C. Huang, K.-C. Yang, H. Lin, T. Tsao, and S.-A. Lee, “Transcriptome alterations of mitochondrial and coagulation function in schizophrenia by cortical sequencing analysis,” *BMC Genomics*, vol. 15, no. Suppl 9, p. S6, 2014.

[4] D.-F. Suen, D. P. Narendra, A. Tanaka, G. Manfredi, and R. J. Youle, “Parkin overexpression selects against a deleterious mtDNA mutation in heteroplasmic cybrid cells,” *Proc. Natl. Acad. Sci.*, vol. 107, no. 26, pp. 11835–11840, Jun. 2010.

[5] D. Hahn, R. A. Kumar, T. E. Ryan, and L. F. Ferreira, “Mitochondrial Respiration and H_2O_2 Emission in Saponin-permeabilized Murine Diaphragm Fibers: Optimization of Fiber Separation and Comparison to Limb Muscle,” *Am. J. Physiol. Physiol.*, p. ajpcell.00184.2019, Jul. 2019.

[6] P. Pasdois, J. E. Parker, E. J. Griffiths, and A. P. Halestrap, “The role of oxidized cytochrome c in regulating mitochondrial reactive oxygen species production and its perturbation in ischaemia.,” *Biochem. J.*, vol. 436, no. 2, pp. 493–505, Jun. 2011.

[7] J. Park *et al.*, “Abnormal Mitochondria in a Non-human Primate Model of MPTP-induced Parkinson’s Disease: Drp1 and CDK5/p25 Signaling,” *Exp. Neurobiol.*, vol. 28, no. 3, p. 414, Jun. 2019.

[8] R. J. Mailloux, S. L. McBride, and M.-E. Harper, “Unearthing the secrets of mitochondrial ROS and glutathione in bioenergetics,” *Trends Biochem. Sci.*, vol. 38, no. 12, pp. 592–602, Dec. 2013.

[9] G. C. Kujoth *et al.*, “Mitochondrial DNA Mutations, Oxidative Stress, and Apoptosis in Mammalian Aging,” *Science (80-.).*, vol. 309, no. 5733, pp. 481–484, Jul. 2005.

[10] O. R. Baris *et al.*, “Mosaic Deficiency in Mitochondrial Oxidative Metabolism Promotes Cardiac Arrhythmia during Aging,” *Cell Metab.*, vol. 21, no. 5, pp. 667–677, May 2015.

[11] A. M. Campbell and C. J. Paradise, *Cellular respiration*. .

[12] “Glycolysis Explained in 10 Easy Steps (With Diagrams),” 2019. [Online]. Available: https://microbiologyinfo.com/glycolysis-10-steps-explained-steps-by-steps-with-diagram/. [Accessed: 18-Jul-2019].

[13] W. W. Chen, E. Freinkman, T. Wang, K. Birsoy, and D. M. Sabatini, “Absolute Quantification of Matrix Metabolites Reveals the Dynamics of Mitochondrial Metabolism,” *Cell*, vol. 166, no. 5, pp. 1324-1337.e11, Aug. 2016.

[14] N. N. Naseri *et al.*, “Abnormalities in the tricarboxylic Acid cycle in Huntington disease and in a Huntington disease mouse model.,” *J. Neuropathol. Exp. Neurol.*, vol. 74, no. 6, pp. 527–37, Jun. 2015.

[15] Y. Yang and A. A. Sauve, “NAD+ metabolism: Bioenergetics, signaling and manipulation for therapy,” *Biochimica et Biophysica Acta - Proteins and Proteomics*, vol. 1864, no. 12. Elsevier B.V., pp. 1787–1800, 01-Dec-2016.

[16] H. Shen *et al.*, “Correlation between normal range of serum alanine aminotransferase level and metabolic syndrome A community-based study,” *Med. (United States)*, vol. 97, no. 41, Oct. 2018.

[17] T. Sarabhai and M. Roden, “Hungry for your alanine: when liver depends on muscle proteolysis.,” *J. Clin. Invest.*, Sep. 2019.

[18] X. Huang *et al.*, “Succinyl-CoA synthetase (SUCLA2) deficiency in two siblings with impaired activity of other mitochondrial oxidative enzymes in skeletal muscle without mitochondrial DNA depletion,” *Mol. Genet. Metab.*, vol. 120, no. 3, pp. 213–222, Mar. 2017.

[19] V. Peters *et al.*, “Formation of 3-hydroxyglutaric acid in glutaric aciduria type I: in vitro participation of medium chain acyl-CoA dehydrogenase,” *JIMD Rep.*, vol. 47, no. 1, pp. 30–34, May 2019.
[20] E. S. Jin, A. D. Sherry, and C. R. Malloy, “Metabolism of glycerol, glucose, and lactate in the citric acid cycle prior to incorporation into hepatic acylglycerols.,” *J. Biol. Chem.*, vol. 288, no. 20, pp. 14488–96, May 2013.
[21] R. J. Rodenburg, “Mitochondrial complex I-linked disease,” *Biochim. Biophys. Acta - Bioenerg.*, vol. 1857, no. 7, pp. 938–945, Jul. 2016.
[22] A. Bender *et al.*, “High levels of mitochondrial DNA deletions in substantia nigra neurons in aging and Parkinson disease,” *Nat. Genet.*, vol. 38, no. 5, pp. 515–517, May 2006.
[23] S. Mehan, V. Monga, M. Rani, R. Dudi, and K. Ghimire, “Neuroprotective effect of solanesol against 3-nitropropionic acid-induced Huntington’s disease-like behavioral, biochemical, and cellular alterations: Restoration of coenzyme-Q10-mediated mitochondrial dysfunction,” *Indian J. Pharmacol.*, vol. 50, no. 6, p. 309, 2018.
[24] L. Fan, Y. Feng, G.-C. Chen, L.-Q. Qin, C. Fu, and L.-H. Chen, “Effects of coenzyme Q10 supplementation on inflammatory markers: A systematic review and meta-analysis of randomized controlled trials,” *Pharmacol. Res.*, vol. 119, pp. 128–136, May 2017.
[25] C. B. Jackson *et al.*, “Mutations in *SDHD* lead to autosomal recessive encephalomyopathy and isolated mitochondrial complex II deficiency,” *J. Med. Genet.*, vol. 51, no. 3, pp. 170–175, Mar. 2014.
[26] S. Hill, K. Sataranatarajan, and H. Van Remmen, “Role of signaling molecules in mitochondrial stress response,” *Frontiers in Genetics*, vol. 9, no. JUL. Frontiers Media S.A., 10-Jul-2018.
[27] S. Wanrooij *et al.*, “In vivo mutagenesis reveals that OriL is essential for mitochondrial DNA replication,” *EMBO Rep.*, vol. 13, no. 12, pp. 1130–1137, Oct. 2012.
[28] S. D. Dyall, M. T. Brown, and P. J. Johnson, “Ancient Invasions: From Endosymbionts to Organelles,” *Science*, vol. 304, no. 5668. pp. 253–257, 09-Apr-2004.
[29] A. G. Iain Johnston and B. P. Williams Correspondence, “Evolutionary Inference across Eukaryotes Identifies Specific Pressures Favoring Mitochondrial Gene Retention Energetic centrality of protein product in complexes dictates gene retention in mtDNA In Brief,” *Cell Syst.*, vol. 2, pp. 101–111, 2016.
[30] T. E. S. Kauppila, J. H. K. Kauppila, and N.-G. Larsson, “Mammalian Mitochondria and Aging: An Update.,” *Cell Metab.*, vol. 25, no. 1, pp. 57–71, Jan. 2017.
[31] D. Harman, “Free radical theory of aging.,” *Mutat. Res.*, vol. 275, no. 3–6, pp. 257–66, Sep. 1992.
[32] J. H. K. Kauppila and J. B. Stewart, “Mitochondrial DNA: Radically free of free-radical driven mutations,” *Biochimica et Biophysica Acta - Bioenergetics*, vol. 1847, no. 11. Elsevier B.V., pp. 1354–1361, 01-Nov-2015.
[33] J. B. Stewart and P. F. Chinnery, “The dynamics of mitochondrial DNA heteroplasmy: implications for human health and disease,” *Nat. Rev. Genet.*, vol. 16, no. 9, pp. 530–542, Sep. 2015.
[34] I. Valenci, L. Yonai, D. Bar-Yaacov, D. Mishmar, and A. Ben-Zvi, “Parkin modulates heteroplasmy of truncated mtDNA in Caenorhabditis elegans,” *Mitochondrion*, vol. 20, pp. 64–70, Jan. 2015.
[35] N. P. Kandul, T. Zhang, B. A. Hay, and M. Guo, “Selective removal of deletion-bearing mitochondrial DNA in heteroplasmic Drosophila.,” *Nat. Commun.*, vol. 7, p. 13100, 2016.
[36] A. N. Bayne and J.-F. Trempe, “Mechanisms of PINK1, ubiquitin and Parkin interactions in mitochondrial quality control and beyond,” *Cell. Mol. Life Sci.*, Jun. 2019.
[37] A. M. Pickrell *et al.*, “Endogenous Parkin Preserves Dopaminergic Substantia Nigral

Neurons following Mitochondrial DNA Mutagenic Stress," *Neuron*, vol. 87, no. 2, pp. 371–381, Jul. 2015.
[38] C. B. Lücking *et al.*, "Association between Early-Onset Parkinson's Disease and Mutations in the *Parkin* Gene," *N. Engl. J. Med.*, vol. 342, no. 21, pp. 1560–1567, May 2000.
[39] W. W. Chen *et al.*, "Inhibition of ATPIF1 Ameliorates Severe Mitochondrial Respiratory Chain Dysfunction in Mammalian Cells," *Cell Rep.*, vol. 7, no. 1, pp. 27–34, Apr. 2014.
[40] M. P. Bayona-Bafaluy, N. Movilla, A. Pérez-Martos, P. Fernández-Silva, and J. A. Enriquez, "Functional genetic analysis of the mammalian mitochondrial DNA encoded peptides: a mutagenesis approach.," *Methods Mol. Biol.*, vol. 457, pp. 379–90, 2008.
[41] G. Twig and O. S. Shirihai, "The Interplay Between Mitochondrial Dynamics and Mitophagy," *Antioxid. Redox Signal.*, vol. 14, no. 10, pp. 1939–1951, May 2011.
[42] D. Wallace *et al.*, "Mitochondrial DNA mutation associated with Leber's hereditary optic neuropathy," *Science (80-.).*, vol. 242, no. 4884, pp. 1427–1430, Dec. 1988.
[43] E. B. Warren, A. E. Aicher, J. P. Fessel, and C. Konradi, "Mitochondrial DNA depletion by ethidium bromide decreases neuronal mitochondrial creatine kinase: Implications for striatal energy metabolism," *PLoS One*, vol. 12, no. 12, Dec. 2017.
[44] D. R. Dunbar, P. A. Moonie, H. T. Jacobs, and I. J. Holt, "Different cellular backgrounds confer a marked advantage to either mutant or wild-type mitochondrial genomes.," *Proc. Natl. Acad. Sci. U. S. A.*, vol. 92, no. 14, pp. 6562–6, Jul. 1995.
[45] M. Yoneda, A. Chomyn, A. Martinuzzi, O. Hurko, and G. Attardi, "Marked replicative advantage of human mtDNA carrying a point mutation that causes the MELAS encephalomyopathy.," *Proc. Natl. Acad. Sci. U. S. A.*, vol. 89, no. 23, pp. 11164–8, Dec. 1992.
[46]. .. A.B..P. van Kuilenburg N. Kamatani, "Purine Metabolism - an overview | ScienceDirect Topics." [Online]. Available: https://www.sciencedirect.com/topics/biochemistry-genetics-and-molecular-biology/purine-metabolism. [Accessed: 29-Sep-2019].
[47] J. Neuzil and M. V Berridge, "Mitochondria break through cellular boundaries," *Aging (Albany. NY).*, Jul. 2019.
[48] L. Liu *et al.*, "Inactivation/deficiency of DHODH induces cell cycle arrest and programed cell death in melanoma," *Oncotarget*, vol. 8, no. 68, pp. 112354–112370, Dec. 2017.
[49] E. T. Kase *et al.*, "Remodeling of Oxidative Energy Metabolism by Galactose Improves Glucose Handling and Metabolic Switching in Human Skeletal Muscle Cells," *PLoS One*, vol. 8, no. 4, Apr. 2013.
[50] C. J. Turner *et al.*, "Systematic segregation to mutant mitochondrial DNA and accompanying loss of mitochondrial DNA in human NT2 teratocarcinoma Cybrids.," *Genetics*, vol. 170, no. 4, pp. 1879–85, Aug. 2005.
[51] H. M. Wilkins, S. M. Carl, and R. H. Swerdlow, "Cytoplasmic hybrid (cybrid) cell lines as a practical model for mitochondriopathies," *Redox Biol.*, vol. 2, pp. 619–631, 2014.
[52] M.-S. Lee, J.-Y. Kim, and S. Y. Park, "Resistance of rho(0) cells against apoptosis.," *Ann. N. Y. Acad. Sci.*, vol. 1011, pp. 146–53, Apr. 2004.
[53] J. S. Takahashi, L. H. Pinto, and M. H. Vitaterna, "Forward and reverse genetic approaches to behavior in the mouse.," *Science*, vol. 264, no. 5166, pp. 1724–33, Jun. 1994.
[54] M. A. Lancaster *et al.*, "Cerebral organoids model human brain development and microcephaly," *Nature*, vol. 501, no. 7467, pp. 373–379, 2013.
[55] C. A. Lino, J. C. Harper, J. P. Carney, and J. A. Timlin, "Delivering crispr: A review of the challenges and approaches," *Drug Delivery*, vol. 25, no. 1. Taylor and Francis Ltd, pp. 1234–1257, 2018.
[56] C. Le and Z. Feng, "Addgene: Zhang Lab's CRISPR Frequently Asked Questions," *Science*, 2013. [Online]. Available: https://www.addgene.org/crispr/zhang/faq/.

[Accessed: 24-Feb-2018].
[57] J. P. Concordet and M. Haeussler, “CRISPOR: Intuitive guide selection for CRISPR/Cas9 genome editing experiments and screens,” *Nucleic Acids Res.*, vol. 46, no. W1, pp. W242–W245, Jul. 2018.
[58] J. D. Arroyo *et al.*, “A Genome-wide CRISPR Death Screen Identifies Genes Essential for Oxidative Phosphorylation.,” *Cell Metab.*, vol. 24, no. 6, pp. 875–885, 2016.
[59] R. Sekine, T. Kawata, and T. Muramoto, “CRISPR/Cas9 mediated targeting of multiple genes in Dictyostelium,” *Sci. Rep.*, vol. 8, no. 1, Dec. 2018.
[60] P. Vladimir *et al.*, “Optimization of Golden Gate assembly through application of ligation sequence-dependent fidelity and bias profiling,” *bioRxiv*, p. 322297, 2018.
[61] V. Potapov *et al.*, “Comprehensive Profiling of Four Base Overhang Ligation Fidelity by T4 DNA Ligase and Application to DNA Assembly,” *ACS Synth. Biol.*, vol. 7, no. 11, pp. 2665–2674, Nov. 2018.
[62] R. Rossignol, B. Faustin, C. Rocher, M. Malgat, J.-P. Mazat, and T. Letellier, “Mitochondrial threshold effects.,” *Biochem. J.*, vol. 370, no. Pt 3, pp. 751–62, Mar. 2003.
[63] N. S. Chandel, “Mitochondria as signaling organelles,” *BMC Biology*, vol. 12. BioMed Central Ltd., 27-May-2014.
[64] M. Saki and A. Prakash, “DNA damage related crosstalk between the nucleus and mitochondria,” *Free Radical Biology and Medicine*, vol. 107. Elsevier Inc., pp. 216–227, 01-Jun-2017.
[65] A. Sallmyr, Y. Matsumoto, V. Roginskaya, B. Van Houten, and A. E. Tomkinson, “Inhibiting mitochondrial DNA ligase IIIα activates caspase 1-dependent apoptosis in cancer cells,” *Cancer Res.*, vol. 76, no. 18, pp. 5431–5441, Sep. 2016.
[66] B. C. Albensi, “What Is Nuclear Factor Kappa B (NF-κB) Doing in and to the Mitochondrion?,” *Front. Cell Dev. Biol.*, vol. 7, Aug. 2019.
[67] M. Zuckermann *et al.*, “A novel cloning strategy for one-step assembly of multiplex CRISPR vectors,” *Sci. Rep.*, vol. 8, no. 1, Dec. 2018.
[68] S. Bae, J. Park, and J. S. Kim, “Cas-OFFinder: A fast and versatile algorithm that searches for potential off-target sites of Cas9 RNA-guided endonucleases,” *Bioinformatics*, vol. 30, no. 10, pp. 1473–1475, May 2014.
[69] M. C. Canver *et al.*, “Integrated design, execution, and analysis of arrayed and pooled CRISPR genome-editing experiments,” *Nat. Protoc.*, vol. 13, no. 5, pp. 946–986, May 2018.
[70] V. Koduri *et al.*, “Peptidic degron for IMiD-induced degradation of heterologous proteins,” *Proc. Natl. Acad. Sci. U. S. A.*, vol. 116, no. 7, pp. 2539–2544, Feb. 2019.
[71] S. A. Gangopadhyay *et al.*, “Precision Control of CRISPR-Cas9 Using Small Molecules and Light,” *Biochemistry*, vol. 58, no. 4. American Chemical Society, pp. 234–244, 29-Jan-2019.
[72] D. Spadafora, N. Kozhukhar, V. N. Chouljenko, K. G. Kousoulas, and M. F. Alexeyev, “Methods for efficient elimination of mitochondrial DNA from cultured cells,” *PLoS One*, vol. 11, no. 5, May 2016.
[73] R. Z. Fayzulin, M. Perez, N. Kozhukhar, D. Spadafora, G. L. Wilson, and M. F. Alexeyev, “A method for mutagenesis of mouse mtDNA and a resource of mouse mtDNA mutations for modeling human pathological conditions,” *Nucleic Acids Res.*, vol. 43, no. 9, pp. e62–e62, May 2015.
[74] N. Fischel-Ghodsian *et al.*, “Mitochondrial gene mutation is a significant predisposing factor in aminoglycoside ototoxicity.,” *Am. J. Otolaryngol.*, vol. 18, no. 3, pp. 173–8.
[75] C.-Y. Tzen, P. Thajeb, T.-Y. Wu, and S.-C. Chen, “Melas with point mutations involving tRNALeu (A3243G) and tRNAGlu(A14693g).,” *Muscle Nerve*, vol. 28, no. 5, pp. 575–81, Nov. 2003.
[76] R. W. Taylor and D. M. Turnbull, “Mitochondrial DNA mutations in human disease.,” *Nat. Rev. Genet.*, vol. 6, no. 5, pp. 389–402, May 2005.

[77] M. Tachibana, T. Kuno, and N. Yaegashi, “Mitochondrial replacement therapy and assisted reproductive technology: A paradigm shift toward treatment of genetic diseases in gametes or in early embryos,” *Reproductive Medicine and Biology*, vol. 17, no. 4. John Wiley and Sons Ltd, pp. 421–433, 01-Oct-2018.
[78] R. J. Castro, “Mitochondrial replacement therapy: the UK and US regulatory landscapes,” *J. Law Biosci.*, vol. 3, no. 3, pp. 726–735, Dec. 2016.
[79] J. Cao, H. Wu, and Z. Li, “Recent perspectives of pediatric mitochondrial diseases (Review),” *Experimental and Therapeutic Medicine*, vol. 15, no. 1. Spandidos Publications, pp. 13–18, 01-Jan-2018.
[80] R. W. Taylor *et al.*, “Mitochondrial DNA mutations in human colonic crypt stem cells,” *J. Clin. Invest.*, vol. 112, no. 9, pp. 1351–1360, Nov. 2003.
[81] A. Trifunovic *et al.*, “Premature ageing in mice expressing defective mitochondrial DNA polymerase,” *Nature*, vol. 429, no. 6990, pp. 417–423, May 2004.
[82] N. A. Khan *et al.*, “mTORC1 Regulates Mitochondrial Integrated Stress Response and Mitochondrial Myopathy Progression,” *Cell Metab.*, vol. 26, no. 2, pp. 419-428.e5, Aug. 2017.

List of Figures

List of Tables

List of Abbreviations

AAVS1 ..... Adeno-associated virus integration site 1
α-KG..... alpha-ketogluterate
ALT ..... alanine aminotransferase
ATP ..... adenosine triphosphate
CFL1 ..... Cofilin 1
CoQ10..... Coenzyme Q10
COX ..... cytochrome c oxidase subunit 6A
CRISPR..... clustered regularly interspaced short palindromic repeats
DEX..... dextrose
DNA ..... desoxyribonucleicacid
FACS ..... fluorescence-activated cell sorting
FAD..... Flavin adenine dinucleotide
FMN ..... flavoin mono nucleotid, flavoinmononucleotid
Gal..... galactose
gDNA ..... genomic DNA
GFP..... green fluorescence protein
HEK..... human embryonic kidney cells
kDa..... kilodaltons
KO..... knockout
LDH..... lactate dehydrogenase
mPTP ..... mitochondrial permeability transition pores
mRNA ..... messenger ribonucleic acid
mtDNA ..... mitochondrial desoxyribonucleic acid
NAD ..... Nicotinamide adenine dinucleotide
OXPHOS..... oxidative phosphorylation system
PCR ..... polymerase chain reaction
PD ..... Parkinson's disease
PDH ..... pyruvate dehydrogenase
POLRMT ..... mitochondrial polymerase
PRPP ..... phosphoribosyl pyrophosphate
RNAi..... ribonucleic acid interference
ROS ..... reactive oxygen species
SCS..... succinyl-CoA synthetase

SCZ.....constraining schizophrenia
SDS..... sodium dodecyl sulfate
SGLT1..... glucose transporter 1
sgRNA..... single guide ribonucleic acid
SOD .....superoxide dismutase